ABSTRACT

HOANG, PHUONG. Supervised Learning in Baseball Pitch Prediction and Hepatitis C Diagnosis. (Under the direction of Hien T. Tran.)

Machine learning is so ubiquitous nowadays that one probably uses it multiple times during the day without realizing it. For example, it is used in web search engines to improve efficiency, by email providers to identify junk emails, and in voice recognition, among others. Machine learning is a powerful tool that can be used to analyze large amount of data to make actionable predictions. Since machine learning uses algorithms that iterate on data, the quality and quantity of training data are important factors for accurate predictions. In particular, the data available for baseball pitch prediction is huge, millions of observations (pitches) each containing more than fifty features. However, the prediction task restricts researchers to working only with the less than ideal features that were measured before the target pitch is thrown. In addition, the presence of noise in pitch type labels makes it even harder to train classifiers. Meanwhile, the dataset for Hepatitis C is fairly small with less than two hundreds observations and 20 features. This disadvantage prevents researchers from removing observations with low quality when building reliable diagnosis models. Hence, prediction problems in the presence of missing features are pervasive in machine learning. This thesis focuses on a number of classification methods and other machine learning tools, and tailor them to address the above issues specifically.

First, in the pitch prediction problem, unlike the current method which suggests a static feature selection algorithm for each pitcher, we propose a novel dynamic feature selection procedure that is shown to be more adaptive for each pitcher in each count. The tradeoff is that the size of training data is reduced dramatically with pitcher-count data segmentation. Thus, we propose a simple heuristic approach for constructing and selecting features to include during training that are shown to surpass this tradeoff, which in turn yields considerable improvement in prediction accuracy.

In the second part of the thesis, we propose a new learning algorithm for Hepatitis C diagnosis that addresses the important issue of class imbalance. Most existing learning algorithms simply ignore the presence of class imbalance due to the lucrative high accuracy that can be easily attained. The current method suggests combining over-sampling (minority class) and weighted cost in Support Vector Machine. Through our research study, however, we were able to show that doing both is unnecessary. We choose only to employ the later

but add the parameter optimization procedure to improve classification performance. Our experimental results show that our proposed method is more accurate and reliable than the existing learning methods.

Supervised Learning in Baseball Pitch Prediction and Hepatitis C Diagnosis

by
Phuong Hoang

A dissertation submitted to the Graduate Faculty of
North Carolina State University
in partial fulfillment of the
requirements for the Degree of
Doctor of Philosophy

Applied Mathematics

Raleigh, North Carolina

2015

APPROVED BY:

Carl Meyer	Negash Medhin
Ernie Stitzinger	Hien T. Tran Chair of Advisory Committee

DEDICATION

This thesis is dedicated to my parents, my wife, my son and Odisg.

BIOGRAPHY

Phuong Hoang was born in Saigon, Vietnam on September 3, 1985. He went to the United States at the age 17 spending a year as an exchange student in Hartford high school, Michigan. In 2005, he started his undergraduate studies at University of Bridgeport, Connecticut in Business Administration before seeing the light and switching to mathematics in the second year. He later transferred to North Carolina State University and earned a B.S. in applied mathematics with financial mathematics concentration in May 2010. During his undergraduate studies, he interned at Sony Ericsson as a software tester on the GPS team. After graduation, he continued on at NC State for graduate school in applied mathematics. During his doctoral studies, he served as a REU graduate assistant for three summers. In his spare time, he manages of an e-commerce store that sells and trades textbooks and household electronics. He is also an avid photographer and has volunteered to be a cameraman on a few research workshops.

ACKNOWLEDGEMENTS

First and foremost, I would like to thank my advisor Dr. Hien Tran for his guidance, encouragement, and support during the past 10 years. I deeply appreciate his great patience and the freedom he gave me to pursue new ideas, many of which were made into this thesis. His enthusiasm, persistence and expertise on research guided me throughout my doctoral study, from brainstorming ideas to doing experiments and writing technical papers, among many other things.

I would also like to thank my thesis committee members, Dr. Carl Meyer, Dr. Negash Medhin, and Dr. Ernie Stitzinger for their valuable feedbacks on this thesis. Especially, Dr. Meyer's fruitful lectures play a big role in keeping my love with applied mathematics.

Special thanks go to my undergraduate advisors Dr. Jeff Scroggs and Dr, Sandra Paur. I consider successful completion of Dr. Paur's analysis courses to be my best achievement in undergraduate study. I also owe to her for guiding me to graduate school and making sure it happens. I would also like to acknowledge Dr. H. T. Banks who provided me with a research fellowship during the third year of my Ph.D. program.

Graduate school would not have been the same with my colleagues Mark Hunnell, Rohit Sivaparasad, Hansi Jiang, Glenn Sidle and George Lankford. Besides our many fun social activities, they were always a useful sounding board when tackling theoretical questions. I wish to thank my former REU students, Michael Hamilton, Joseph Murray and Shar Shuai. Mentoring those who are smarter than I am has helped me in many ways, especially in finding better solution for a "solved" problem by looking at them from a different angle. Thanks also go to the research mentors from MIT Lincoln Laboratory Dr. Lori Layne and Dr. David Padgett for whom I was lucky enough to work with for two summers.

There are many friends who have helped me immeasurably throughout my student life. A few deserve special recognition. Nhat-Minh Phan who helped me in scrapping data that I used in this thesis and Nam Tran was always there for me, whether helping me financially during the rainy day or "shipping" his wife to Raleigh to help my wife and babysit my son when I were away for conferences. Particular thanks also go to Quoc Nguyen and Thanh Nguyen for putting up with me throughout the years. Also I would like to thank Dung Tran and Sombat Southivorarat for being excellent readers of this thesis.

My biggest thanks go to my loving and supportive parents, my wife and my son. This thesis is dedicated to them. Thank you for sharing this journey with me.

TABLE OF CONTENTS

LIST OF TABLES

LIST OF FIGURES

CHAPTER

1

INTRODUCTION

1.1 Statement of the Problems

In this thesis, we address some challenges in supervised learning when dealing with both large and small datasets in the context of baseball pitch prediction and medical diagnosis domains. The purpose of this dissertation is to address some major issues that come up with each problem. For pitch prediction, the challenge is finding better alternatives for pitch prediction when only pre-pitch information is available in training. Furthermore, pitchers tend to develop similar pitching patterns at the same pitch count. So instead of having one learning model per pitcher, having a separate model for each pitcher-count pair may adapt to the changes in game situation better. This further data segmentation indeed divides the number of observations available for training classifier into smaller sets. This brings us back to the previous challenge, how to find features with higher predictive strength to compensate for the potential lack of training data. We propose in this thesis an

approach that will overcome this shortcoming. More specifically, from the raw data, we generate synthetic features that replicate human (pitchers) decision making, then group them in their similarity and perform two filtering steps to include only a set of optimal features that are then used for training classifiers. In validation, we applied our final model to other datasets that were unseen by the machine to ensure its effectiveness in predicting future data.

For Hepatitis C diagnosis, researchers have been developing methods for disease classification where nearly perfect (above 95%) accuracy were reached. Many of these studies however omit the presence of class imbalance where accuracy alone is a poor evaluation metric. Some studies use validation method, but report only the best result, another misleading measurement of classification performance with particularly small number of training observations. We propose a method that (1) provides a simpler solution that outperforms the current methods and (2) employs parameters optimization and cross validation within metrics designated for treating class imbalance.

The essence of our methods is to attain the best fit of the (in-sample) data at hand and perform reliably with the out-of-sample data once they encountered (i.e., minimize overfitting possibilities). To achieve this goal, we carefully examine theoretical foundation of overfitting, modify our classifier appropriately and provide as much theoretical justification to the observed heuristic as possible.

1.2 Dissertation Outline

The thesis begins, in Chapter 2, with an introduction of the supervised learning and three classification techniques used later in this study. Chapter 3 follows with the discussion of the overfitting problem in supervised learning, as well as two useful tools to address the overfitting problem. In Chapter 4 we propose a pitch prediction model, built on PITCHf/x data of MLB seasons 2008-2012. We also compare the performance of various classification methods mentioned and employ cross validation techniques that previously introduced in Chapter 2 and 3. Chapter 5 focuses on the medical diagnosis applications in which we reconfigure the Support Vector Machine classification with weighted cost and employ parameters optimization and conduct a wide range of validation techniques to address

the overfitting and to enhance the performance overall. Chapter 6 draws conclusions and suggests areas of potential interest for future work.

1.3 Summary of Contributions

This section summarizes the contributions of this study and refers to the specific sections of the thesis where they can be found:

1. We design and implement a novel feature selection approach for baseball pitch prediction (section 4.3). Our model is shown to adapt well to the different pitchers (section 4.4.3) and different count situation (section 4.4.2) even at the time they change their pitch type. Overall, our experimental results show that our model (1) can achieve higher accuracy (up to 10 %) than the existing method under hold-out validation (introduced in section 3.2.1) and (2) shown to be stable with low variances in cross validation results (less than 2% difference).

2. We propose a new disease diagnosis system that is able to combat overfitting caused by unbalanced datasets. Our model adapts the Support Vector Machine (SVM) method using modified cost function that is sensitive to class imbalance (section 5.3.2). We implement cross validation within the grid search algorithm to determine the best choices of parameters C and γ of the SVM with Gaussian kernel (section 5.3.3). For each classifier, we make 500 simulation runs to measure and compare consistency in term of variances.

CHAPTER

2

CLASSIFICATION

Classification is the process of taking an unlabeled data observation and using some rule or decision-making process to assign a label to it. Given $\mathscr{X}$ is the input space and $\mathscr{Y}$ is the output space (often called labels), $\mathscr{D}$ denotes the data set of input-output examples $(x_1, y_1), ...(x_N, y_N)$ where $y_i = f(x_i)$ for $i = 1, ..., N$. The process of classification is to find an algorithm or strategy that uses the data set $\mathscr{D}$ to find a function g from the hypothesis set H that best approximates the ideal function $f : \mathscr{X} \rightarrow \mathscr{Y}$ [1].

To support this concept, in [1], the authors present the credit card approval example. The goal here is for the bank to use historical records of previous customers to figure out a good formula for credit approval. In this case, as illustrated in Figure 2.1, x_i is the customer information that is used to make a credit decision, y_i is a Yes/No decision, f is the ideal formula for credit approval and data set $\mathscr{D}$ contains all input-output examples corresponding to previous customers and the credit decision for them in hindsight. Once we find g (f remains unknown) that best matches f on the training data, we apply g to classify new credit card customer with the hope that it would still match f on (future)

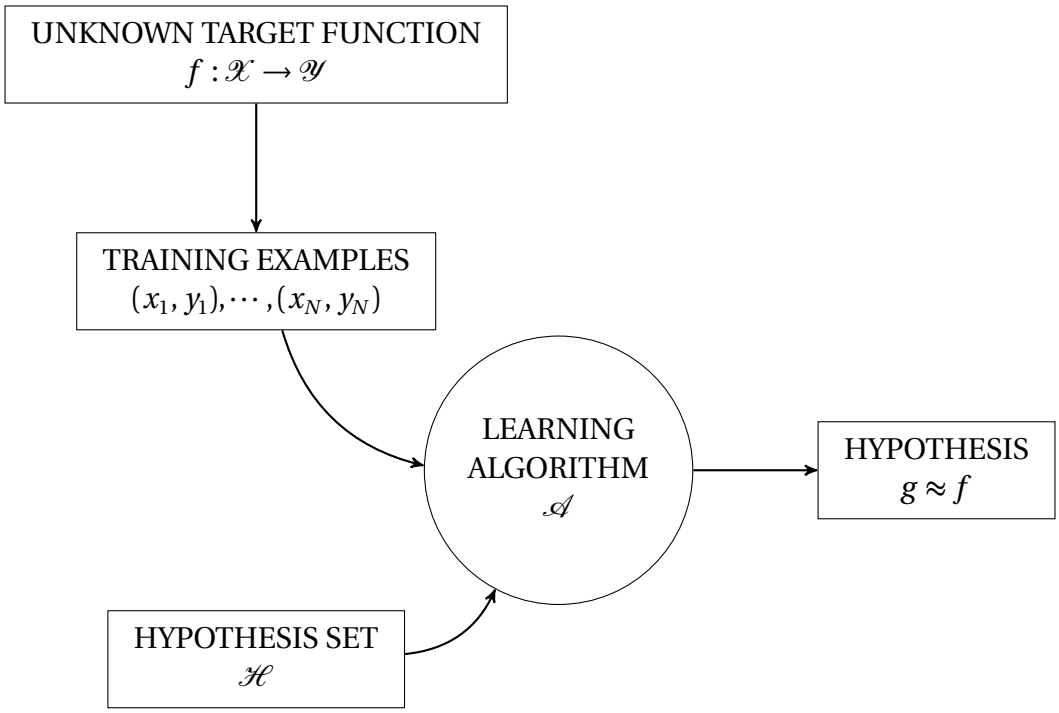

Figure 2.1: Basic setup of the learning problem [1]

unlabeled data. The notation used in this chapter and the next one mainly follow that of [1], some frequently used notation are listed in Table 2.1.

Table 2.1: Frequently Used Notation, adapted from [1, 12, 37, 57]

λ	regularization parameter
Ω	penalty for model complexity; either a bound on generalization error, or a regularization term
Φ	feature transform, $z = \Phi(x)$
ϕ	a coordinate in feature transform Φ, $z = \phi_i(x)$
C	bound on the size of weights in a soft order constraint
d	dimensionality of the in put space $\mathscr{X} = \mathbb{R}^d$ or $\mathscr{X} = \{1\} \times \mathbb{R}^d$
$\mathscr{D}$	data set $\mathscr{D} = \{(x_1, y_i), ..., (x_N, y_N)\}$ often the training set, but sometimes split into training and validation/test sets
$\mathscr{D}_{\text{train}}$	subset of $\mathscr{D}$ used for training when a validation or test set is used
E_{in}, $E_{\text{in}}(h)$	in-sample error (training error) for hypothesis h
E_{cv}	cross validation error
E_{out}, $E_{\text{out}}(h)$	out-of-sample error for hypothesis h
E_{val}	validation error
E_{test}	test error
f	target function, $f : \mathscr{X} \to \mathscr{Y}$
g	final hypothesis $g \in \mathscr{H}$ selected by the learning algorithm; $g : \mathscr{X} \to \mathscr{Y}$
$g^{(\mathscr{D})}$	final hypothesis when the training set is $\mathscr{D}$
h	a hypothesis $h \in H$; $h : \mathscr{X} \to \mathscr{Y}$
$\mathscr{H}$	hypothesis set
$\mathscr{X}$	input space whose elements are $x \in \mathscr{X}$
$\mathscr{Y}$	output space whose elements are $y \in \mathscr{Y}$

The classification methods used in this study are the k-nearest neighbors (k-NN), the Linear Discriminant Analysis (LDA) and the Support Vector Machine (SVM). A brief description of k-NN and LDA is provided in the next two sections. Meanwhile SVM is chosen to be the main classifier of our study and we will discuss it in more details in the third section.

2.1 k-Nearest Neighbors

The k-nearest neighbors algorithm (k-NN) classifies an unlabeled point based on the closest k training points in the multidimensional feature space; each of the k neighbors has a class label and the label of a given point is determined by the majority vote of the class labels of its k-nearest neighbors, see [57]. An example of k-NN is presented below in Figure 2.2.

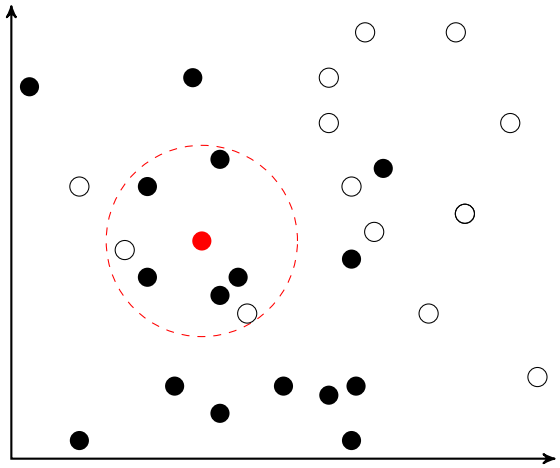

Figure 2.2: An example of k-NN; using the 7-NN rule, the unknown data point in red is classified to the black class. Out of the seven nearest neighbors, five are of black class and two are of white class (the dashed circle denotes the region that contains the 7 nearest neighbors of the unknown data point).

1. A value for k is defined by the user.
2. The distance between the unclassified point and each class-labeled point is calculated.
3. The k nearest neighbors are chosen based on that distance.
4. The class label of the unclassified point is defined as the majority of the class labels of the k nearest neighbors.

This method is customizable—the user can use different values of k and optionally pick different distance metrics. The standard choice of metric is the Euclidean distance (2.1),

$$d_{\text{Eucl}}(x,y) = \sum_{i=1}^{l} (x_i - y_i)^2. \tag{2.1}$$

Mahalanobis distance (2.2) takes into account the correlations of the data,

$$d^{\,i}_{\text{Mahal}}(x,y) = \sqrt{(x - y^T \Sigma^{-1} (x-y)}, \tag{2.2}$$

where Σ is the covariance [9, 57]. It is clear that if the covariance matrix Σ is the identity matrix, then Mahalanobis distance is the same as the Euclidean distance. Another common metric often used with k-NN is the Manhattan distance (2.3) ,also known as the city-block distance or L_1 norm,

$$d_{\text{Man}}(x,y) = \sum_{i=1}^{l} |x_i - y_i|. \tag{2.3}$$

An example of a binary class problem using k-NN classifier is presented below. In this example, data from both classes are generated from the Gaussian distribution with different means and covariances, as illustrated in Figure 2.3. We use the k-NN algorithm with three metrics above to classify the unknown data set (black). The unknown set distributes similar to class 2 but its center is closer to that of class 1. As shown in Table 2.2, Mahalanobis outperforms the other two types of distance in this case because it pays more attention to the covariances of each class. However the drawback is the time complexity due to matrix multiplication.

Table 2.2: Accuracy and speed comparison of k-NN method using different metrics

Methods	Accuracy	CPU time
k-NN	97.80	0.039014s
k-NN Man	97.90	0.039674s
k-NN Mahal	98.40	0.174085s

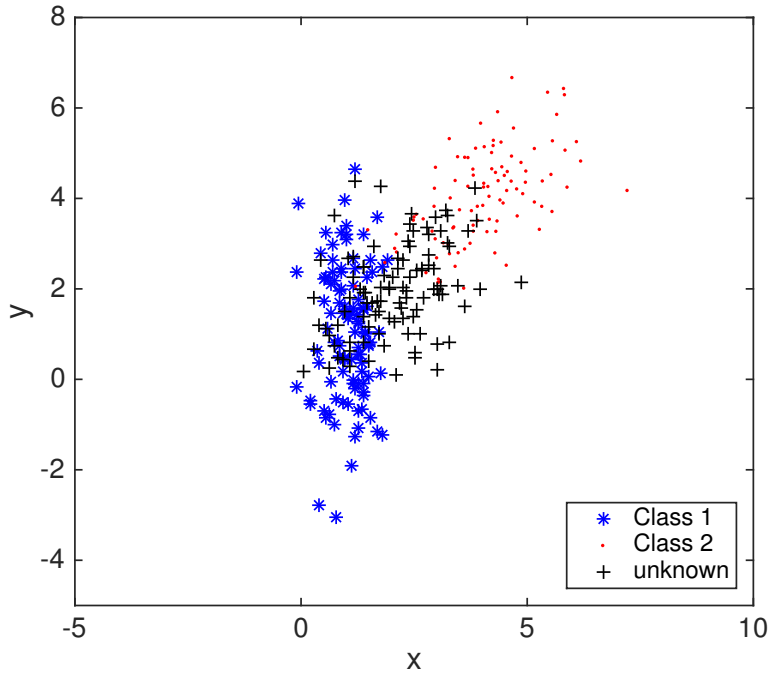

Figure 2.3: An example of binary classification problem. Data from class 1 (blue) favor the y-axis while data from class 2 (red) spread out the along the North East direction. The unknown data (black) is to be classified with k-NN.

2.2 Linear Discriminant Analysis

The Linear Discriminant Analysis (LDA) classifier assumes that the observations within each class k are generated from a Gaussian (or normal) distribution with a class-specific mean vector μ_k's and a common variance σ_k^2's. Estimates for these parameters are substituted into the Bayes classifier results.

Assume that we have only one feature (or predictor) in a K-class classification problem. Then the Bayes' theorem states that

$$\Pr(Y = k|X = x) = \frac{\pi_k f_k(x)}{\sum_{l=1}^{K} \pi_l f_l(x)}, \tag{2.4}$$

where π_k represent the prior probability that a randomly chosen observation is associated with the k-th class, $f_k(X) \equiv \Pr(X = x|Y = k)$ denotes the density function of X for an observation that comes from k-th class, and $\Pr(Y = k|X)$, abbreviated as $p_k(X)$, refers to the posterior probability that an observation $X = x$ belongs to the k-th class. If we can compute all the terms for (2.4), we would then easily classify an observation to the class for which $p_k(X)$ is largest.

Since $f_k(x)$ is Gaussian, the normal density takes the form

$$f_k(x) = \frac{1}{\sqrt{2\pi}\sigma_k} \exp\left(-\frac{1}{2\sigma_k^2}\left(x-\mu_k\right)^2\right). \tag{2.5}$$

Substituting (2.5) into (2.4) under assumption that $\sigma_k^2 \equiv \sigma^2$, we obtain

$$p_k(x) = \frac{\pi_k \frac{1}{2\pi\sigma} \exp\left(-\frac{1}{2\sigma^2}\left(x-\mu_k\right)^2\right)}{\sum_{l=1}^{K} \pi_l \frac{1}{2\pi\sigma} \exp\left(-\frac{1}{2\sigma^2}\left(x-\mu_l\right)^2\right)} \tag{2.6}$$

$$= \frac{\pi_k \exp\left(-\frac{1}{2\sigma^2}\left(x-\mu_k\right)^2\right)}{\sum_{l=1}^{K} \pi_l \exp\left(-\frac{1}{2\sigma^2}\left(x-\mu_l\right)^2\right)}. \tag{2.7}$$

To classify an observation $X = x$, we need to see which of the $p_k(x)$ is largest. Taking the

log of (2.7), we obtain

$$\log\big(p_k(x)\big) = \log\left(\pi_k \exp\left(-\frac{1}{2\sigma^2}\big(x-\mu_k\big)^2\right)\right) - \underbrace{\log\left(\sum_{l=1}^{K}\pi_l \exp\left(-\frac{1}{2\sigma^2}\big(x-\mu_l\big)^2\right)\right)}_{\text{this term does not depend on } k}. \tag{2.8}$$

Notice that $\log\big(p_k(X)\big)$ depends only on the first term of the right hand side. Let's call this term $\eta_k(x)$, we have

$$\eta_k(x) = \log\left(\pi_k \exp\left(-\frac{1}{2\sigma^2}\big(x-\mu_k\big)^2\right)\right) \tag{2.9}$$

$$= \log(\pi_k) - \frac{1}{2\sigma^2}\big(x-\mu_k\big)^2 \tag{2.10}$$

$$= \log(\pi_k) - \underbrace{\frac{x^2}{2\sigma^2}}_{\text{this term does not depend on } k} + x\cdot\frac{\mu_k}{\sigma^2} - \frac{\mu_k^2}{2\sigma^2}. \tag{2.11}$$

Therefore, classifying an observation $X = x$ is equivalent to assigning it to the class which

$$\delta_k(x) = x\cdot\frac{\mu_k}{\sigma^2} - \frac{\mu_k^2}{2\sigma^2} + \log(\pi_k) \tag{2.12}$$

is largest, where $\delta_k(x)$ denotes the class discriminant function.

An example is shown in Figure 2.4, adapted from [33]. The two normal density functions are shown, $f_1(x)$ and $f_2(x)$, represent two distinct classes. The mean and variance parameters for the two density functions are $\mu_1 = 40$, $\mu_2 = 80$, and $\sigma_1^2 = \sigma_2^2 = 100$. Because the two densities overlap, there is some uncertainty about the class to which a given observation $X = x$ belongs. Under the assumption that an observation is equally likely come from either class, $\pi_1 = \pi_2 = 0.5$, then we can compute the Bayes classifier since X is drawn from a Gaussian distribution within each class, and all parameters involved are known. In practice, even if we are certain on the assumption that X is drawn from a Gaussian distribution within each class, we still have to estimate the parameters μ_k, π_k, and σ^2. This is where the LDA method comes into play, it specifically provides the estimates for μ_k, π_k, and σ^2, and hence, an approximation of Bayes classifier. Since these estimates depend largely on the training data that may or may not be the a good representation of each class, the LDA

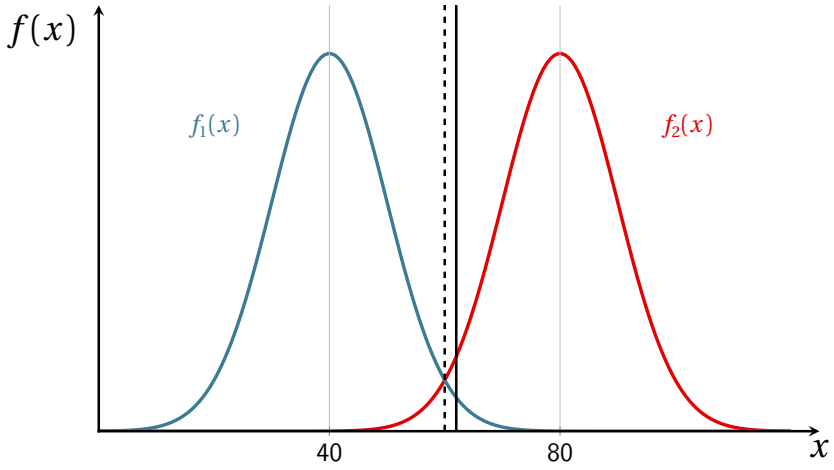

Figure 2.4: An example of LDA. Two one-dimensional density functions are shown. The dashed vertical line represents the Bayes decision boundary. The solid vertical line represents the LDA decision boundary estimated from training data. The source code used to make this figure is adapted from [58], used under CC0 1.0, via Wikimedia Commons.

decision boundary can be different from the Bayes decision boundary, as illustrated in Figure2.4.

The LDA method approximates the Bayes classifier by substituting the following estimates for π_k, μ_k and σ^2 into (2.12),

$$\begin{aligned}
\hat{\pi}_k &= \frac{n_k}{n}, \\
\hat{\mu}_k &= \frac{1}{n_k} \sum_{i:y_i=k} x_i, \\
\hat{\sigma}^2 &= \frac{1}{n-K} \sum_{k=1}^{K} \sum_{i:y_i=k} (x_i - \hat{\mu}_k)^2,
\end{aligned}$$

where n is the total number of training observations and n_k is the number of training observations in k-th class. After the LDA procedure, (2.12) becomes

$$\hat{\delta}_k(x) = x \cdot \frac{\hat{\mu}_k}{\hat{\sigma}^2} - \frac{\hat{\mu}_k^2}{2\hat{\sigma}^2} + \log(\hat{\pi}_k). \tag{2.13}$$

The LDA classifier can be extended to multiple predictors. To do this, we assume that $X = (X_1, X_2, ..., X_p)$ is drawn from a multivariate Gaussian distribution with a class-specific mean vector and common covariance matrix, the corresponding equations (2.5) and (2.12) are

$$f(x) = \frac{1}{(2\pi)^{p/2}|\Sigma|^{1/2}} \exp\left(-\frac{1}{2}(x-\mu)^T \Sigma^{-1}(x-\mu)\right), \tag{2.14}$$

and

$$\delta_k(x) = x^T \Sigma^{-1}\mu_k - \frac{1}{2}\mu_k^T \Sigma^{-1}\mu_k + \log(\pi_k). \tag{2.15}$$

The formulas for estimating the unknown parameters π_k, μ_k, and Σ are similar to the one-dimensional case. To assign an observation $X = x$, the LDA uses these estimates in (2.15) and assigns the class label for which discrimination function $\hat{\delta}_k(x)$ is largest. The word *linear* in the classifier's name comes from the fact that these discrimination functions are linear functions of x. Unlike the k-NN, where no assumptions are made about the shape of the decision boundary, the LDA produces linear decision boundaries. See [33] for more details.

2.3 Support Vector Machines

2.3.1 Linear Separable Case

Support Vector Machine is a linear classification tool that simultaneously optimizes prediction accuracy and avoids overfitting (Chapter 3). The algorithm is dependent on the notion of margin.

For a two-class classification problem, the separating hyperplane

$$u(x) = w \cdot x + b \tag{2.16}$$

is not unique as it may be biased towards one class [1]. The goal is to maximize the distance between two classes, and effectively drawing the decision boundary that maximizes this margin. Intuitively, this separation is achieved by the hyperplane that has the largest distance to the nearest training data point (the so-called *support vectors*) of either class.

[1] the dot symbol in (2.16) denotes the inner product

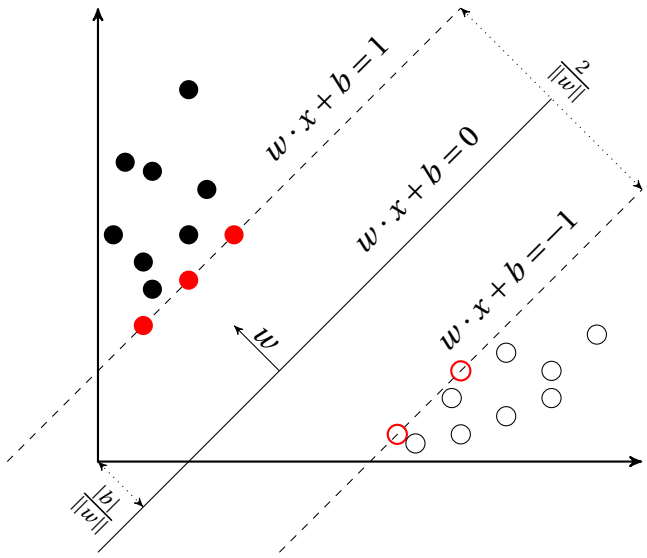

Figure 2.5: An example of a linearly separable two-class problem with SVM. The source code used to make this figure is adapted from [51].

An example of linearly separable SVM for binary classification is presented in Figure 2.5.

Let $\{x_i, y_i\}$, $i = 1, 2, ..., l$, $x_i \in \mathbb{R}^d$ be the input-output samples of the training set, D. Suppose we have some separating hyperplane H, a point x that lies on H needs to satisfy $w \cdot x + b = 0$, where w is the weight vector that is normal to H. Then all observations from the training data need to satisfy the constraints

$$x_i \cdot w + b \geq +1 \quad \text{if } y_i = +1, \tag{2.17}$$

$$x_i \cdot w + b \leq -1 \quad \text{if } y_i = -1, \tag{2.18}$$

which can be simplified to

$$y_i(x_i \cdot w + b) \geq 1, \quad i = 1, 2. \tag{2.19}$$

We define the following hyperplanes,

$$\begin{aligned} H_1 &: x_i \cdot w + b = +1, \\ H_2 &: x_i \cdot w + b = -1, \end{aligned} \tag{2.20}$$

such that the points on the planes H_1 and H_2 are the support vectors. Note that H_1 and H_2 have same normal vector hence they are parallel to each other. In addition, no training points should lie between them. Now, from (2.20) the distances from the origin to H_1 and H_2 are $\frac{|1-b|}{||w||}$ and $\frac{|-1-b|}{||w||}$, respectively. Hence, the margin between H_1 and H_2 is $\frac{2}{||w||}$. In order to maximize the margin between H_1 and H_2, $||w||$ must be minimized. Combining this with the constraint (2.19), we have an optimization problem

$$\min \quad \frac{1}{2}||w||^2, \tag{2.21}$$

$$\text{subject to} \quad y_i(x_i w + b) \geq 1, \quad i = 1, 2, ..., l. \tag{2.22}$$

Since the norm $||w||$ involves a square root, which makes optimization difficult, we have replaced $||w||$ with $\frac{||w||^2}{2}$. We now have a quadratic program that can be solved using Lagrange multipliers, as suggested in [14, 57, 60]. The Lagrangian for this problem is

$$L = \frac{1}{2}||w||^2 - \sum_{i=1}^{l} \alpha_i [y_i(x_i \cdot w + b) - 1], \tag{2.23}$$

where α_i denotes the Lagrangian multipliers. To minimize L, the following Karush-Kuhn-Tucker (KKT) conditions [57] must be satisfied

$$L_w = 0, \tag{2.24}$$

$$L_b = 0, \tag{2.25}$$

$$\alpha_i \geq 0, \quad i = 1, 2, ..., l, \tag{2.26}$$

$$\alpha_i [y_i(x_i \cdot w + b) - 1] = 0, \quad i = 1, 2, ..., l. \tag{2.27}$$

Combining these with equation (2.23) we have

$$w = \sum_{i=1}^{l} \alpha_i y_i x_i, \tag{2.28}$$

$$\sum_{i=1}^{l} \alpha_i y_i = 0. \tag{2.29}$$

We now consider the Lagrangian duality problem which is called the Wolfe dual representation form. Following [14, 57], we have,

$$\max \quad \frac{1}{2}||w||^2 - \sum_{i=1}^{l} \alpha_i [y_i(x_i \cdot w + b) - 1], \tag{2.30}$$

$$\text{subject to} \quad w = \sum_{i=1}^{l} \alpha_i y_i x_i, \tag{2.31}$$

$$\sum_{i=1}^{l} \alpha_i y_i = 0, \tag{2.32}$$

$$\alpha_i \geq 0. \tag{2.33}$$

Substituting (2.31) in (2.30) yields

$$\frac{1}{2}\left(\sum_{i=1}^{l} \alpha_i y_i x_i\right) \cdot \left(\sum_{j=1}^{l} \alpha_j y_j x_j\right) - \left(\left(\sum_{i=1}^{l} \alpha_i y_i x_i\right) \cdot \left(\sum_{j=1}^{l} \alpha_j y_j x_j\right) + b \sum_{i=1}^{l} \alpha_i y_i - \sum_{i=1}^{l} \alpha_i\right). \tag{2.34}$$

Applying (2.32) and rearranging the terms, we have

$$\sum_{i=1}^{l} \alpha_i - \frac{1}{2}\left(\sum_{i=1}^{l} \alpha_i y_i x_i\right) \cdot \left(\sum_{j=1}^{l} \alpha_j y_j x_j\right). \tag{2.35}$$

The Lagrangian problem becomes

$$\max \quad \sum_{i=1}^{l} \alpha_i - \frac{1}{2} \sum_{i,j=1} \alpha_i \alpha_j y_i y_j x_i \cdot x_j, \tag{2.36}$$

$$\text{subject to} \quad \sum_{i=1}^{l} \alpha_i y_i = 0, \tag{2.37}$$

$$\alpha_i \geq 0. \tag{2.38}$$

If $\alpha_i > 0$, the corresponding data point is the support vector and the solution for the optimal separating hyperplane is

$$w = \sum_{i=1}^{n} \alpha_i y_i x_i, \tag{2.39}$$

where $n \leq l$ is the number of support vectors. Once we determine w and b, from equation (2.27), the optimal linear discriminant function is

$$g(x) = \text{sgn}(w \cdot x + b) \tag{2.40}$$

$$= \text{sgn}\left(\sum_{i=1}^{l} \alpha_i y_i x_i \cdot x + b \right). \tag{2.41}$$

Finally, from equation (2.27), for any nonzero α_m which is associated with some support

vector x_m and label y_m, we compute b as followed

$$\alpha_m[y_m(x_m \cdot w + b) - 1] = 0, \tag{2.42}$$

$$y_m(x_m \cdot w + b) - 1 = 0, \tag{2.43}$$

$$y_m x_m \cdot w + y_m b - 1 = 0, \tag{2.44}$$

$$b = \frac{1}{y_m}(1 - y_m x_m w), \tag{2.45}$$

$$= \frac{1}{y_m} - x_m \cdot w, \tag{2.46}$$

$$= \frac{1}{y_m} - \sum_{i=1}^{l} \alpha_i y_i x_i \cdot x_m, \tag{2.47}$$

$$= y_m - \sum_{i=1}^{l} \alpha_i y_i x_i \cdot x_m. \tag{2.48}$$

Notice that equation (2.48) holds because $y_m = \pm 1$.

2.3.2 Nonseparable Case - Soft Margin SVM

The above setup only works for separable data. For a nonseparable two-class problem, we cannot draw a separating hyperplane with associated hyperplanes H_1 and H_2 such that there is no data point lying between them. To address this issue, recall that H_1 and H_2 have the form

$$x_i \cdot w + b = \pm 1 \tag{2.49}$$

and the margin is the distance between them. Any training data point, x_i (with associated class label y_i) in the training set must belong to one of the following three cases (see Figure 2.6),

- x_i lies outside the margin and correctly classified, so x satisfies the inequality constraints in (2.22), i.e., $y_i(x_i \cdot w + b) \geq 1$,
- x_i lies between the margin and correctly classified, so $0 \leq y_i(x_i \cdot w + b) < 1$,
- x_i lies between the margin and incorrectly classified, so $y_i(x_i \cdot w + b) < 0$.

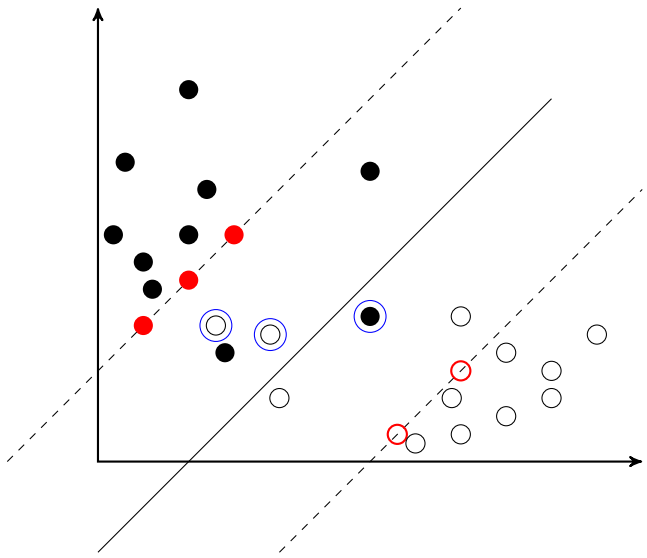

Figure 2.6: An example of a linearly nonseparable two-class problem with SVM. The incorrectly classified data points are enclosed in blue circle. The source code used to make this figure is adapted from [51].

By introducing a slack variable ξ_i, we account all the above three cases in a single constraint

$$y_i(x \cdot w + b) \geq 1 - \xi_i. \tag{2.50}$$

That is, the first, second, and third case correspond to $\xi_i = 0$, $0 < \xi_i \leq 1$, and $\xi_i > 1$ respectively. The constraints (2.17) and (2.51) become

$$x_i \cdot w + b \geq +1 - \xi_i \quad \text{if} \quad y_i = +1, \tag{2.51}$$

$$x_i \cdot w + b \leq -1 + \xi_i \quad \text{if} \quad y_i = -1. \tag{2.52}$$

The new optimization problem is

$$\begin{aligned} \min \quad & \frac{1}{2}||w||^2 + C\sum_{i=1}^{l}\xi_i, \\ \text{subject to} \quad & y_i(x_i w + b) \geq 1 - \xi_i, \quad i = 1,2,...,l, \\ & \xi_i \geq 0, \quad i = 1,2,...,l, \end{aligned} \tag{2.53}$$

where C is a parameter that controls the trade-off between the two main goals: maximizing margin and having fewer number of misclassification. This is still a convex optimization problem, hence we proceed with the Lagrange method as before [57]. The Lagrangian for this new problem is

$$L = \frac{1}{2}||w||^2 + C\sum_{i=1}^{l}\xi_i - \sum_{i=1}^{l}\mu_i\xi_i - \sum_{i=1}^{l}\alpha_i[y_i(x_i \cdot w + b) - 1 + \xi_i], \tag{2.54}$$

with the corresponding KKT conditions

$$L_w = 0 \quad \text{or} \quad w = \sum_{i=1}^{l}\alpha_i y_i x_i, \tag{2.55}$$

$$L_b = 0 \quad \text{or} \quad \sum_{i=1}^{l}\alpha_i y_i = 0, \tag{2.56}$$

$$L_{\xi_i} = 0 \quad \text{or} \quad C - \mu_i - \alpha_i = 0, \quad i = 1,2,...,l, \tag{2.57}$$

$$\alpha_i[y_i(x_i \cdot w + b) - 1 + \xi_i] = 0, \quad i = 1,2,...,l, \tag{2.58}$$

$$\mu_i\xi_i = 0, \quad i = 1,2,...,l, \tag{2.59}$$

$$\alpha_i \geq 0, \quad i = 1,2,...,l, \tag{2.60}$$

$$\mu_i \geq 0, \quad i = 1,2,...,l, \tag{2.61}$$

and the associated Wolfe dual representation

$$\max \quad \frac{1}{2}||w||^2 + C\sum_{i=1}^{l}\xi_i - \sum_{i=1}^{l}\mu_i\xi_i - \sum_{i=1}^{l}\alpha_i[y_i(x_i\cdot w+b)-1+\xi_i], \tag{2.62}$$

$$\text{subject to} \quad w = \sum_{i=1}^{l}\alpha_i y_i x_i, \tag{2.63}$$

$$\sum_{i=1}^{l}\alpha_i y_i = 0, \tag{2.64}$$

$$C-\mu_i-\alpha_i = 0, \quad i = 1,2,...,l, \tag{2.65}$$

$$\alpha_i \geq 0, \quad \mu_i \geq 0, \quad i = 1,2,...,l. \tag{2.66}$$

By substituting the equality constraints (2.63) and (2.64) into the Lagrangian (2.62), the optimization problem becomes

$$\max \quad \sum_{i=1}^{l}\alpha_i - \frac{1}{2}\sum_{i,j=1}\alpha_i\alpha_j y_i y_j x_i\cdot x_j, \tag{2.67}$$

$$\text{subject to} \quad \sum_{i=1}^{l}\alpha_i y_i = 0, \tag{2.68}$$

$$0 \leq \alpha_i \leq C, \quad i = 1,2,...,l. \tag{2.69}$$

As before, we use KKT conditions, equations (2.58) and (2.59) to solve for b. Combining equation (2.57), $C-\alpha_i-\mu_i = 0$ and equation (2.59), $\mu_i\xi_i = 0$ in show that $\xi_i = 0$ if $\alpha_i < C$. Therefore we simply take any point that satisfies $0 < \alpha_i < C$ and $\xi_i = 0$, and using equation (2.58) to compute b. With some algebra, we should obtain the solution for b that is identical to equation (2.48) from the separable case in the previous section. Once α, w, and b are determined, we obtain the optimal decision function

$$g(x) = \text{sgn}\left(\sum_{i=1}^{l}\alpha_i y_i x_i\cdot x + b\right), \tag{2.70}$$

$$\text{where} \quad b = y_m - \sum_{i=1}^{l}\alpha_i y_i x_i\cdot x_m. \tag{2.71}$$

This decision function is identical to equation (2.41) of the separable case with the only exception that the Lagrange multipliers α_i are now bounded above by C, as seen in (2.69) [14].

2.3.3 Nonlinearly Separable Case - Kernel trick

In reality, the two classes cannot be linearly separated. Fortunately, there is a simple method that makes the linear SVM work well with non-linear case. The idea relies on the kernel trick that allows us to map the original input space to a higher-dimensional features space where the training set can be linearly separable [18, 57]. Figure 2.7 illustrates the linear separability of the kernel trick.

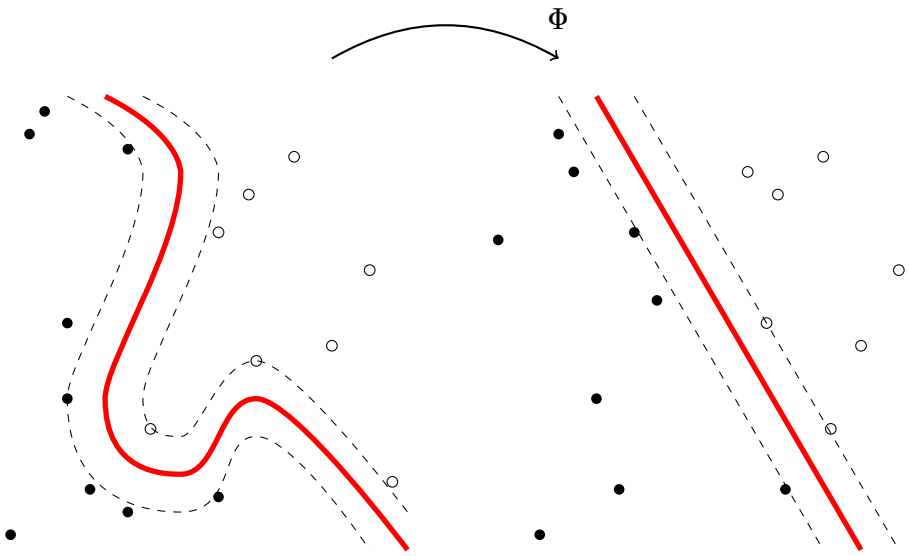

Figure 2.7: Kernels are used for mapping a non-linearly separable problem into a higher dimension linearly separable problem. The source code used to make this figure is adapted from [50].

To see how does mapping to a higher dimensional space provide linearly separability, let's consider an example shown in Figure 2.8. Data points from the red class and the black class in Figure 2.8a cannot simply linearly separated in the original space $\mathscr{X} = \mathbb{R}^2$. Under

the mapping

$$\Phi : \mathbb{R}^2 \to \mathbb{R}^3, \qquad \Phi(x) = \begin{pmatrix} x_1 \\ x_2 \\ x_1 x_2 \end{pmatrix}, \tag{2.72}$$

the two classes can be linearly separated by the xy- hyperplane, as shown in Figure 2.8b.

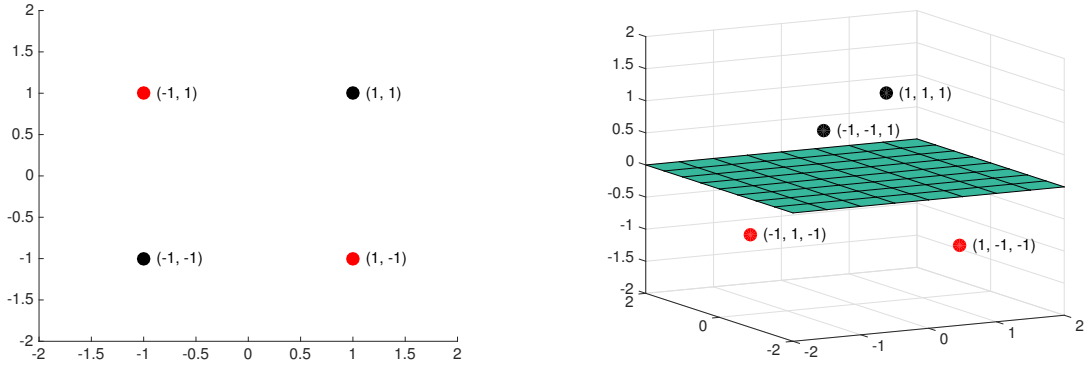

(a) Input space $\mathcal{X} = \mathbb{R}^2$ (b) Feature space $\mathcal{H} = \mathbb{R}^3$

Figure 2.8: An example of kernel trick.

The most widely used kernels in practice are:

$$\text{Linear kernel} \qquad K(x_i, x_j) = x_i \cdot x_j, \tag{2.73}$$

$$\text{Polynomial kernel} \qquad K(x_i, x_j) = (r + \gamma x_i \cdot x_j)^p, \tag{2.74}$$

$$\text{Gaussian kernel} \qquad K(x_i, x_j) = \exp(-\gamma ||x_i - x_j||^2), \tag{2.75}$$

$$\text{Sigmoid kernel} \qquad K(x_i, x_j) = \tanh(r + \gamma x_i \cdot x_j). \tag{2.76}$$

If we have an learning algorithm where examples (training data) appear only in the inner products, we can freely replace the inner product with a different one, so called kernel, where the kernel happens to be an inner product in some feature space. Remember the soft margin SVM in (section 2.3.2) in which examples enter the training algorithm in the

form of inner product, via equations (2.67) - (2.69),

$$\begin{aligned} \max \quad & \sum_{i=1}^{l} \alpha_i - \frac{1}{2} \sum_{i,j=1} \alpha_i \alpha_j y_i y_j \underbrace{x_i \cdot x_j}_{\text{inner product}}, \\ \text{subject to} \quad & \sum_{i=1}^{l} \alpha_i y_i = 0, \\ & 0 \leq \alpha_i \leq C. \end{aligned}$$

Suppose we map the data to some higher dimensional Euclidean space $\mathscr{H}$, using a mapping Φ such that

$$\Phi : \mathbb{R}^d \rightarrow \mathscr{H}, \tag{2.77}$$

then the SVM algorithm depends only on the data through the inner product in $\mathscr{H}$ by $\Phi(x_i) \cdot \Phi(x_j)$. Moreover, if there exists a kernel function K such that

$$K(x_i, x_j) = \Phi(x_i) \cdot \Phi(x_j), \tag{2.78}$$

then replacing the inner product by the kernel $K(x_i, x_j)$, the Wolfe dual representation becomes

$$\max \quad \sum_{i=1}^{l} \alpha_i - \frac{1}{2} \sum_{i,j=1} \alpha_i \alpha_j y_i y_j \underbrace{K(x_i, x_j)}_{\text{kernel}}, \tag{2.79}$$

$$\text{subject to} \quad \sum_{i=1}^{l} \alpha_i y_i = 0, \tag{2.80}$$

$$0 \leq \alpha_i \leq C, \quad i = 1, 2, ..., l \tag{2.81}$$

and the solution has form

$$g(x) = \operatorname{sgn}\left(\sum_{i=1}^{l} \alpha_i y_i K(x_i, x) + b\right), \tag{2.82}$$

$$\text{where} \quad b = y_m - \sum_{i=1}^{l} \alpha_i y_i K(x_i, x_m), \tag{2.83}$$

for some support vector x_m with label y_m, associated with nonzero Lagrangian multiplier α_m and $\xi_m = 0$. It should be noted that the entire learning SVM algorithm does not require either the higher dimensional space $\mathscr{H}$ or the mapping Φ explicitly but the solution to the optimization problem is still a simple linear combination. That is the beauty of kernel trick.

For a given kernel, not only that computing the associated Φ and $\mathscr{H}$ is irrelevant, both Φ and $\mathscr{H}$ can also be non-unique. For example, suppose that $x \in \mathbb{R}^2$, we choose a simple polynomial kernel $K(x_i, x_j) = (x_i \cdot x_j)^2$ corresponding to (2.74) with $r = 0$, $p = 2$, and $\gamma = 1$. We can find the mapping Φ

$$\Phi : \mathbb{R}^2 \to \mathscr{H}, \tag{2.84}$$

$$\langle \Phi(x), \Phi(y) \rangle = (x \cdot y)^2. \tag{2.85}$$

Here, it's easy to show that all the mappings Φ_1, Φ_2 and Φ_3 and the associated feature spaces $\mathscr{H}_1 = \mathscr{H}_2 = \mathbb{R}^3$, and $\mathscr{H}_3 = \mathbb{R}^4$ satisfy condition (2.85). That is, neither the mapping Φ nor the space $\mathscr{H}$ is unique for this given kernel [14].

$$\Phi_1(x) = \begin{pmatrix} x_1^2 \\ \sqrt{2} x_1 x_2 \\ x_2^2 \end{pmatrix}, \quad \Phi_2(x) = \frac{1}{\sqrt{2}} \begin{pmatrix} (x_1^2 - x_2^2) \\ 2 x_1 x_2 \\ (x_1 + x_2)^2 \end{pmatrix}, \quad \Phi_3(x) = \begin{pmatrix} x_1^2 \\ x_1 x_2 \\ x_1 x_2 \\ x_2^2 \end{pmatrix}.$$

It also should be noted that the Gaussian kernel (2.75) can be infinite dimensional. To show this, we need to find a corresponding $\Phi \in \mathbb{R}^\infty$ for kernel (2.75). Without loss of generality, assume $\gamma > 0$ and $x \in \mathbb{R}$. Expanding the exponential term as the Taylor series,

we have

$$
\begin{aligned}
K(x_i, x_j) &= \exp(-\gamma ||x_i - x_j||^2) \\
&= \exp(-\gamma (x_i - x_j)^2) \\
&= \exp(-\gamma x_i^2 + 2\gamma x_i x_j - \gamma x_j^2) \\
&= \exp(-\gamma x_i^2) \exp(-\gamma x_j^2) \exp(2\gamma x_i x_j) \\
&= \exp(-\gamma x_i^2) \exp(-\gamma x_j^2) \left(\sum_{k=0}^{\infty} \frac{\left(2\gamma x_i x_j\right)^k}{k!} \right) \\
&= \sum_{k=0}^{\infty} \left(\exp(-\gamma x_i^2) \sqrt{\frac{\left(2\gamma\right)^k}{k!}} x_i^k \ \exp(-\gamma x_j^2) \sqrt{\frac{\left(2\gamma\right)^k}{k!}} x_j^k \right) \\
&= \Phi(x_i) \cdot \Phi(x_j),
\end{aligned}
$$

where

$$
\Phi(x) = \exp(-\gamma x^2) \left(1, \sqrt{\frac{2\gamma}{1!}} x, \sqrt{\frac{(2\gamma)^2}{2!}} x^2, \sqrt{\frac{(2\gamma)^3}{3!}} x^3, \cdots \right)^T.
$$

That is, Φ maps $x \in \mathbb{R}^1$ to $\mathbb{R}^\infty$.

In order to determine which kernels does there exist a pair $(\Phi, \mathscr{H})$ with the desired properties, we rely on the Mercer's condition. In general, any positive semi-definite function that satisfies the Mercer's condition (see Theorem[2] 2.3.1 below) can be used as a kernel function [12, 18, 37, 57].

Theorem 2.3.1 *(Mercer's Theorem [22, 59]) There exists a mapping* Φ *and an expansion*

$$
K(x, y) = \sum_i \Phi(x)_i \Phi(y)_i \tag{2.86}
$$

[2] Proof of Mercer's theorem is presented in [22, 59].

if and only if, for any $g(x)$ such that

$$\int g(x)^2 \, dx \quad \textit{is finite} \tag{2.87}$$

then

$$\int K(x,y)g(x)g(y) \, dx \, dy \geq 0. \tag{2.88}$$

Let's apply the above theorem to check if the the dot product $K(x,y) = (x \cdot y)^p$ is a valid kernel. We must show that for any $g(x)$ satisfying (2.87),

$$\int \left(\sum_{i=1}^{d} x_i y_i \right)^p g(x)g(y) \, dx \, dy \geq 0. \tag{2.89}$$

As suggested in [14], a typical term in the expansion of $\left(\sum_{i=1}^{d} x_i y_i \right)^p$ contributes a term of the form

$$\frac{p!}{r_1!r_2!\cdots(p-r_1-r_2\cdots)!} \int x_1^{r_1} x_2^{r_2} \cdots y_1^{r_1} y_2^{r_2} \cdots g(x)g(y) \, dx \, dy, \tag{2.90}$$

to the left hand side of (2.88). This term is equivalent to

$$\frac{p!}{r_1!r_2!\cdots(p-r_1-r_2\cdots)!} \left(\int x_1^{r_1} x_2^{r_2} \cdots g(x) \, dx \right)^2 \geq 0. \tag{2.91}$$

Kernel construction is an active field of machine learning research [1, 14, 57], however, it does not belong to the scope of this study. We employ only the existing ones such as the linear kernel (SVM-L) and Gaussian kernel (SVM-G) in our experiments with SVM.

CHAPTER

3

OVERFITTING

Overfitting is the phenomenon where a hypothesis with lower in-sample error E_{in} yields a higher out-of-sample error E_{out}. In this case, E_{in} is no longer useful in choosing the hypothesis that best represents the target function. Often it is the case when the model is more complex than necessary, as Abu-Mostafa (2012) put, "it uses additional degrees of freedom to fit idiosyncrasies (noise), yielding a final hypothesis that is inferior" [1]. An example of overfitting is illustrated in Figure 3.1. Overfitting can also occurs when a hypothesis that is far simpler than the target function, hence it is referred as underfitting [1].

Overfitting mainly depends on the three parameters: the noise σ^2, the target function complexity Q_f, and the number of training data points N. As σ^2 increases, more stochastic noise[2] is added to the data. Meanwhile, as Q_f increases, we add more deterministic noise[3] to

[1] We will examine this special case in detail in chapter 5

[2] When learning from data, there are random fluctuations and/or measurements errors in the data which cannot be modeled. This phenomenon is referred to the stochastic noise.

[3] For a given learning problem, there is a best approximation to the target function, the part of the target function outside this best fit acts like noise in the data. This model's inability to approximate f is referred to

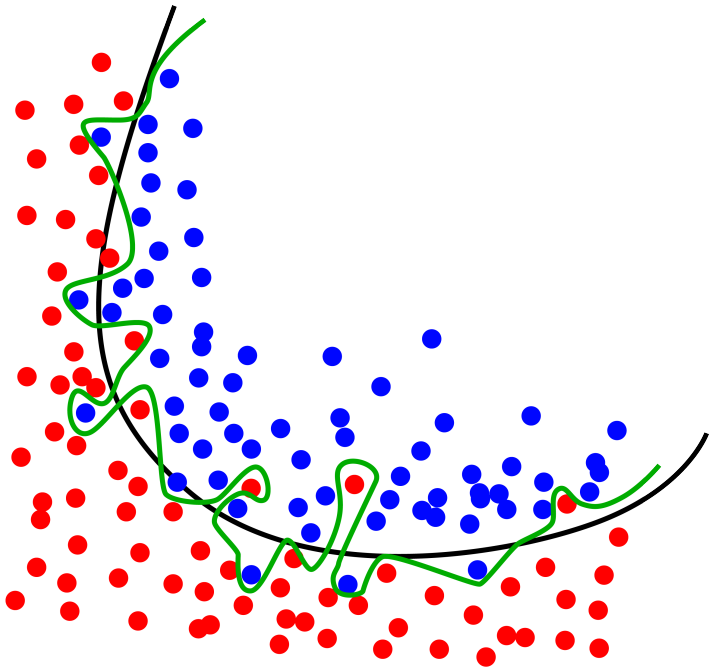

Figure 3.1: Example showing overfittting of a classifier by Chabacano, used under CC BY-SA, via Wikimedia Commons [17]. The green curve separates the blue and the red dots perfectly in this (training) data set, hence it has lower E_{in} than that of the black curve. However, it also models the noise at the boundary in addition to model the underlying trend. Hence, it will more likely perform poorly on a new data set from the same population, has higher E_{out}. The green curve is an example of an overfitted classifier.

the data. As the number of data points N increases, noise level σ^2 drops and less overfitting occurs. It is important to realize that both stochastic and deterministic noises cannot be modeled and cannot be distinguished [1]. To understand how these two types of noise affect the model performance, one could use the bias-variance decomposition of error (loss) function:

$$E_{\mathscr{D}}[E_{\text{out}}] = \sigma^2 + \text{bias} + \text{var}. \tag{3.1}$$

In equation (3.1), σ^2 and **bias** are the direct impact of the stochastic noise and deterministic noise, respectively. The interesting **var** term is indirectly impacted by both types of the noise, through the hypothesis set $\mathscr{H}$. Because **var** is controlled by the size of $\mathscr{H}$, it decreases as the number of data points N increases. Moreover, if we make $\mathscr{H}$ more complex, we will decrease **bias** in the expense of increasing **var**. In practice, the later usually dominates, so overfitting occurs not because of the direct impact on noise, but mainly because of the indirect impact on variance. In this chapter, we mainly adapt the context of Chapter 4 in [1] which gives a throughout discussion to the topic of overfitting and the methodology to prevent overfitting.

3.1 Regularization

Regularization is used to prevent overfitting by explicitly controlling the model complexity. To achieve this goal, an additional parameter $\Omega(h)$ is introduced to account for model complexity of an individual hypothesis h. As shown in the error function (3.2), instead of minimizing $E_{\text{in}}(h)$ alone, one would minimizes both $E_{\text{in}}(h)$ and $\Omega(h)$. By doing this, the learning algorithm is constrained to not only fitting the data well but also using a simpler hypothesis hence improves generalization [1, 12].

$$E_{\text{out}}(h) \leq E_{\text{in}}(h) + \Omega(\mathscr{H}) \quad \text{for all} \quad h \in \mathscr{H}. \tag{3.2}$$

Several regularization techniques have been presented in the machine learning literature. Some notable ones are weight decay [1], L1 and L2 regularization in regression [48], and Tikhonov regularization [12]. We emphasize on the last technique, most commonly

the deterministic noise.

used for ill-posed problems and widely adapted in statistics and machine learning. For example, the author of [11] proves that training with noise is equivalent to solving a Tikhonov regularization with Neural Network classifier. We will also see how it can be viewed as a soft constraint SVM problem.

In the simplest case, given a mapping $A : X \to Y$, to obtain a regularized solution to $Ax = y$, we seek for x that fits y in the least squares sense, but penalize solutions of large norm and solve the optimization problem

$$\begin{aligned} x_\lambda &= \arg\min ||Ax - y||_Y^2 + \lambda ||x||_X^2, \\ &= (A^*A + \lambda I)^{-1} A^* y, \end{aligned} \tag{3.3}$$

where $\lambda > 0$ is called the regularization parameter.

Back to the supervised learning regime, given n input-output examples $(x_1, y_1), ..., (x_n, y_n)$ with $x_i \in \mathbb{R}^d$ and $y_i \in \{-1, 1\}$ for all i, we want to choose a classifier function $f : \mathscr{X} \to \mathscr{Y}$ that fits the data but not too complex. Tikhonov regularization (3.3) suggests such function as follows:

$$\min_{f \in \mathscr{H}} \quad \frac{1}{n} \sum_{i=1}^{n} V(y_i, f(x_i)) + \lambda ||f||_{\mathscr{H}}^2, \tag{3.4}$$

where $V : \mathscr{Y} \times \mathscr{Y} \to \mathbb{R}$ is the loss function, $||\cdot||_{\mathscr{H}}$ is the norm on the hypothesis space of functions $\mathscr{H}$, and $\lambda \in R$ is the regularization parameter [55]. The most intuitive loss function is indeed the missclassifiation loss function, i.e, the 0-1 loss, which gives 0 if we have classified correctly, $f(x_i)$ and y_i have the same sign, and 1 if incorrectly classified. This forms a step function

$$V(y_i, f(x_i)) = \begin{cases} 1 & \text{for} \quad y_i f(x_i) < 0, \\ 0 & \text{for} \quad y_i f(x_i) \geq 0. \end{cases} \tag{3.5}$$

The major drawback is that the step function (3.5) is non convex (also undefined at $x = 0$), which gain difficulties in the optimization problem [1, 55, 57]. To address this shortcoming, one can use the *hinge loss* function. In particular, the *hinge loss* function assigns a positive loss to *correct* classification in such $0 < y_i f(x_i) < 1$, as shown in Figure 3.2. The goal is to classify most input x_i with at least a value of $y_i f(x_i) \geq 1$. It's analogous

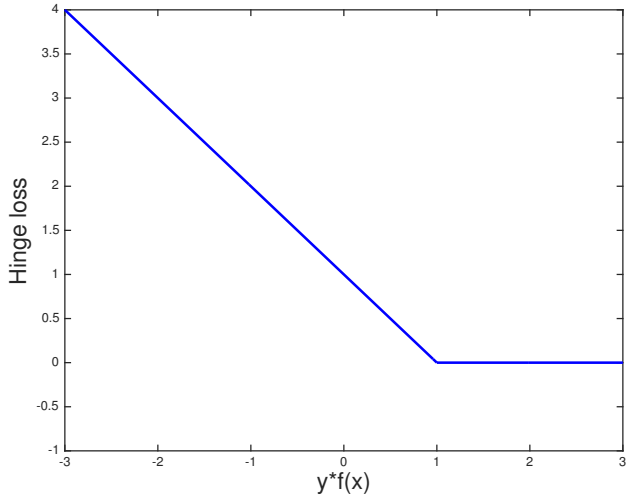

Figure 3.2: Hinge loss function. Note that the loss is asymmetric: incorrect classification, $y_i f(x_i) < 0$, is linearly increasing loss as $y_i f(x_i)$ decreases and correct classification with $y_i f(x_i) \geq 1$ is always zero loss.

to the idea of SVM when we want to classifies most of x_i outside of the separating margin. Now, given the hinge-loss function, Tikhonov regularization becomes

$$\min_{f \in H} \quad \frac{1}{n} \sum_{i=1}^{n} (1 - y_i f(x_i))_+ + \lambda ||f||_H^2, \tag{3.6}$$

where $(u)_+ = \max\{u, 0\}$. Multiplying (3.6) by $\frac{1}{2\lambda}$ and choosing $C = \frac{1}{2n\lambda}$ yield

$$\min_{f \in H} \quad \frac{1}{2} ||f||_H^2 + C \sum_{i=1}^{n} (1 - y_i f(x_i))_+. \tag{3.7}$$

Note that the hinge loss is not differentiable at $y_i f(x_i) = 1$. To address this issue, let's introduce slack variables ξ_i such that for each point in the training set, ξ_i replace $(1 - y_i f(x_i)$.

For each ξ_i, we require $\xi_i \geq (1 - y_i f(x_i))_+$. The Tikhonov regularization problem becomes

$$\begin{aligned} \min_{f \in H} \quad & \frac{1}{2}\|f\|_H^2 + C\sum_{i=1}^{n} \xi_i, \\ \text{subject to} \quad & y_i f(x_i) \geq 1 - \xi_i, \quad i = 1, ..., n, \\ & \xi_i \geq 0, \end{aligned} \tag{3.8}$$

which is equivalent to the SVM problem (2.53) in Section 2.3. For a more comprehensive explanation of regularization perspective on SVM, see [11, 14, 55, 57].

3.2 Validation

In the previous section, we show that regularization can combat overfitting by control model complexity. Validation on the other hand estimates the out-of-sample error directly, as illustrated in (3.9). Note that both techniques are often used together in a learning problem as an attempt to minimizing E_{out} rather than just E_{in}.

$$\begin{aligned} E_{\text{out}}(h) &= E_{\text{in}}(h) + \underbrace{\text{overfit penalty}}_{\text{regularization estimates this quantity}}, \\ \underbrace{E_{\text{out}}(h)}_{\text{validation estimates this quantity}} &= E_{\text{in}}(h) + \text{overfit penalty}. \end{aligned} \tag{3.9}$$

The process of validation requires the presence of the validation set. But first let's define the test set. The test set is a subset of input space $\mathscr{D}$ that is removed from the data set. The test set is absolutely not involved in the learning process, hence unlike E_{in}, E_{test} is an unbiased estimation of E_{out}. The validation set is constructed similarly, it is also a subset of $\mathscr{D}$ that is not used directly in the training process. However, the validation error, E_{val}, is used to help us make certain choices in choosing parameters of a classifier or feature selection. This indirectly impacts the learning process rendering the validation set no longer qualified to be a test set. Nevertheless, E_{val} is still a better choice than E_{in} in term of bias for model evaluation.

3.2.1 Hold-Out Validation

Hold-out method involves randomly partition the dataset $\mathscr{D}$ of size N into two parts: a training set $\mathscr{D}_{\text{train}}$ of size $(N-K)$ and a validation set (or hold out-set) $\mathscr{D}_{\text{val}}$ of size K. The learning model is trained on the $\mathscr{D}_{\text{train}}$ to obtain a final hypothesis g^- that is later used to predict the responses for the observations in the $\mathscr{D}_{\text{val}}$ [4]. The validation error for g^- is computed using the validation set $\mathscr{D}_{\text{val}}$ as follows,

$$E_{\text{val}} = \frac{1}{K} \sum_{x_n \in \mathscr{D}_{\text{val}}} \text{e}\big(g^-(x_n), y_n\big), \tag{3.10}$$

where $\text{e}\big(g^-(x), y\big)$ denotes the point-wise error function,

$$\text{e}\big(g^-(x), y\big) = \begin{cases} 0 & \text{for} \quad g^-(x) = y, \\ 1 & \text{for} \quad \text{otherwise.} \end{cases} \tag{3.11}$$

It is important to realize that the validation error rate E_{val} gives an unbiased estimate of E_{out} because the hypothesis g^- was formed independently of the data point in $\mathscr{D}_{\text{val}}$. In fact, taking expectation of E_{val} with respect to $\mathscr{D}_{\text{val}}$, results in

$$\mathbb{E}_{\mathscr{D}_{\text{val}}}\big[E_{\text{val}}(g^-)\big] = \frac{1}{K} \sum_{x_n \in \mathscr{D}_{\text{val}}} \mathbb{E}_{\mathscr{D}_{\text{val}}}\big[\text{e}\big(g^-(x_n), y_n\big)\big], \tag{3.12}$$

$$= \frac{1}{K} \sum_{x_n \in \mathscr{D}_{\text{val}}} \mathbb{E}_{x_n}\big[\text{e}\big(g^-(x_n), y_n\big)\big], \tag{3.13}$$

$$= \frac{1}{K} \sum_{x_n \in \mathscr{D}_{\text{val}}} E_{\text{out}}(g), \tag{3.14}$$

$$= E_{\text{out}}(g^-). \tag{3.15}$$

The first equality in (3.12) uses linearity of expectation and the second equality in (3.13) is true because $\text{e}\big(g^-(x_n), y_n\big)$ depends only on x_n. Hold-out method is a very simple strategy but it has two drawbacks: (1) the test error E_{out} can be greatly varying depending on which

[4] The minus subscript in g^- indicates that some data points have been removed from the training (for validation purpose. At the end g is the final hypothesis that is trained with all data points in $\mathscr{D}_{\text{train}}$.

observations are included in the training and validation set; and (2) only a subset of the available observations are used for training and validating the model, so we can potentially lose valuable information especially with smaller datasets [37].

3.2.2 Cross Validation

In the validation process, finding K, the size of the validation set is not easy. The dilemma we encounter is described in (3.16). In the first approximation, we want K to be small, to minimize the difference between $E_{\text{out}}(g)$ and $E_{\text{out}}(g^-)$. However, in the second approximation, larger K results in less variance between $E_{\text{out}}(g^-)$ and $E_{\text{val}}(g^-)$.

$$E_{\text{out}}(g) \underset{\text{small } K}{\approx} E_{\text{out}}(g^-) \underset{\text{large } K}{\approx} E_{\text{val}}(g^-) \tag{3.16}$$

This leads us to a refinement of the hold-out approach, called cross validation (CV), a common strategy for model selection that gained widespread application due to its simplicity and universality.

The popularity of the cross validation technique is mostly due to the universality of the data splitting heuristics [8]. In the basic approach, called k-fold cross-validation, the original sample is randomly partitioned into k equal size subsamples. Commonly, $k = 10$ is considered standard CV, another choice when $k = N$ so $K = 1$ is referred as *leave-one-out* approach. Of the k subsamples, a single subsample is retained as the validation data for testing the model, and the remaining $k-1$ subsamples are used as training data. The cross-validation process is then repeated k times (the folds), with each of the k subsamples used exactly once as the validation data. The k results from the folds can then be averaged (or otherwise combined) to produce a single estimation of the true error rate. That is,

$$E_{\text{cv}}(g^-) = \frac{1}{k}\sum_{n=1}^{k} \mathrm{E}_{\text{val}}(g_n^-). \tag{3.17}$$

The advantage of this method is that all observations are used for both training and validation, and each observation is used for validation exactly once. Not only does k-fold CV give a nearly unbiased estimate of the generalized (out-of-sample) error rate, it also reduces the variability in the estimation, hence considered better than the hold-out method

in term of avoiding overfitting [37]. However it often produce unpredictable high variability on small dataset. Efron, Bradley (1983) shows that applying randomized bootstrap (a nonparametric maximum likelihood estimation) can enhance the stability of regular CV [27]. Furthermore, Andrew Ng (1996) points out that overfitting can occur even with large dataset that is partially corrupted by noise. The author shows that it can be overcome by selecting the hypothesis with a higher CV error, over others with lower CV errors and propose an algorithm (LOOCVCV [5]) to perform this task.

[5] LOOCVCV: Leave-one-out Cross-Validated Cross Validation

CHAPTER

4

BASEBALL PITCH PREDICTION

Baseball, one of the most popular sports in the world, has a uniquely discrete gameplay structure that naturally allows fans and observers to record information about the game in progress, resulting in a wealth of data that is available for analysis. Major League Baseball (MLB), the professional baseball league in the US and Canada, uses a system known as PITCHf/x to record information about every individual pitch that is thrown in league play. We apply several machine learning classification methods to this data to classify pitches by type (fastball or nonfastball). We then extend the classification to prediction by restricting our analysis to pre-pitch features. By performing significant feature analysis and introducing a dynamic approach for feature selection, moderate improvement over published results is achieved.

4.1 PITCHf/x Data

In this study, a database created by Sportvision's PITCHf/x pitch tracking system that characterizes each pitch with approximately 50 features in which 18 features from the raw data are used directly (see Table 4.1). Additional features are derived from the raw data that we believe to be more relevant to pitch prediction. The motivation for our approach is that prediction, unlike classification, relies on pre-delivery game information. For example, post-delivery features such as speed and curve angle, which can be used to determine whether or not it was a fastball, are not available pre-pitch. So for prediction, we use information from prior pitches in similar game plan situation to judge which pitch can be expected. Some of the adaptive features include the percentage of fastballs thrown in the previous inning, the velocity of the previous pitch, strike result percentage of the previous pitch, and current game count. Overall, we developed a set of 77 features and arranged them into 6 groups of similarity. Group 1 contains features that describe general information of the current game situation such as inning, number of outs, number of base runners, etc. Group 2 features focus on pitch type tendency of the pitcher, such as percentage of fastballs thrown in the previous inning, in previous game, or lifetime percentage of fastballs, etc. Group 3 features aggregate pitch velocity information from the past, while group 4 concerns the location of previous pitches as they cross the home plate. Group 5 consists of features that illustrate different ways to measure *strike result percentage* in a given situation while group 6 does the same for *ball-strike combo* from the similar count in the past. For a full list of features used in each of the 6 groups, see Appendix A.1. In addition, a glossary of baseball terminologies is provided in Appendix A.2.

4.2 Related Work

One area of statistical analysis of baseball that has gained attention in the last decade is pitch analysis. Studying pitch characterisitcs allows baseball teams to develop more successful pitching routines and batting strategies. To aid this study, baseball pitch data produced by the PITCHf/x system is now widely available for both public and private use. PITCHf/x is a pitch tracking system that allows measurements to be recorded and associated

Table 4.1: List of original attributes selected for pitch prediction

PITCHf/x Variables	**Description**
atbat_num	number of pitches recorded against the specific batter he is facing
outs	number of outs during the at bat
batter	batter's unique identification number
pitcher	pitcher's unique identification number
stand	dominant hand of batter; left/right
p_throws	pitching hand of pitcher; left/right
des	outcome of one pitch from pitcher's perspective; ball/strike/foul/in play, etc.
event	outcome of at bat from batter's perspective; ground out/double/single/walk, etc
pitch_type	classification of pitch type; FF = Four-seam Fastball, SL = Slider, etc.
sv_id	date/time stamp of the pitch; YYMMDD_ hhmmss
start_speed	pitch speed, miles per hour
px	horizontal distance of the pitch from the home plate
pz	vertical distance, of the pitch from the home plate
on_first	binary column; display 1 if runner on first, 0 otherwise
on_second	binary column; display 1 if runner on second, 0 otherwise
on_third	binary column; display 1 if runner on third, 0 otherwise
type_confidence	likelihood of the pitch type being correctly classified
ball_strike	display either ball or strike

with every pitch thrown in Major League Baseball (MLB) games. The system, which was installed in every MLB stadium circa 2006, records useful information for every pitch. Some measurements such as the initial velocity, plate velocity, release point, spin angle and spin rate are useful to characterize the pitch type (e.g., fastball, curveball, changeup, knuckleball). The pitch type is determined by PITCHf/x using a proprietary classification algorithm. Because of the large number of MLB games in a season (2430) and the high number of pitches thrown in a game (an average of 146 pitches per team), PITCHf/x provides a rich data set on which to train and evaluate methodologies for pitch classification and prediction. Pitch analysis can either be performed using the measurements provided by PITCHf/x in their raw form or by using data derived features. Each of the recorded pitches is classified by the PITCHf/x proprietary algorithm and provided with measurement data. For the purposes of analysis, the proprietary PITCHf/x classification algorithm is assumed to generally represent truth. For example, in [9] and [10], several classification algorithms including Support Vector Machine (SVM) and Bayesian classifiers were used to classify pitch types based on features derived from PITCHf/x data. The authors evaluated classification algorithms both on accuracy, as compared to the truth classes provided by PITCHf/x, and speed. In addition, Linear Discrimination Analysis (LDA) and Principal Component Analysis (PCA) were used to evaluate feature dimension reduction useful for classification. The pitch classification was evaluated using a set of pitchers' data from the 2011 MLB regular season.

Another important area of ongoing research is pitch prediction, which could have significant real-world applications and potentially provides MLB managers with the statistical competitive edge in simulation using in training and coaching. One example of research on this topic is the work by [31], who use a Linear Support Vector Machine (SVM-L) to perform binary (*fastball* vs. *nonfastball*) classification on pitches of unknown type. The SVM-L model is trained on PITCHf/x data from pitches thrown in 2008 and tested on data from 2009. Across all pitchers, an average prediction accuracy of roughly 70 percent is obtained, though pitcher specific accuracies vary.

Other related pitch data analysis in the literature, such as [65], which examines the pitching strategy of major league pitchers, specifically determining whether or not they (from a game theoretic approach) implement optimally mixed strategies for handling batters. The paper concludes that pitchers do mix optimally with respect to the *pitch*

variable and behave rationally relative to the result of any given pitch.

Our study provides a machine learning approach to pitch prediction, using a binary classification method to predict pitch type, defined as *fastball* vs. *nonfastball*. A distinct difference in our approach is the introduction of an adaptive strategy to feature selection to mimic portions of pitchers' behavior. This allows the machine learning algorithm to select different sets of features in different situations to train the classifiers. The features used contain not only original features, but also hybrid features that are created to better resemble the way pitchers seem to process data. Additionally, cross validation is implemented to detect and avoid overfitting in our predictions. Overall, the prediction accuracy is improved by approximately 8% from results published in [31]. A report of our initial effort in this study can be found in [32].

4.3 Our Model

4.3.1 Dynamic Feature Selection Approach

A key difference between our approach and former research of [31] is the feature selection methodology. Rather than using a static set of features, an adaptive set is used for each pitcher/count pair. This allows the algorithm to adapt to achieve the best prediction performance result possible on each pitcher/count pair of data.

In baseball there are a number of factors that influence a pitcher's decision, either consciously or unconsciously. For example, one pitcher may not like to throw curveballs during the daytime because the increased visibility makes them easier to spot; however, another pitcher may not make his pitching decisions based on the time of the game. In order to maximize accuracy of a prediction model, one must try to accommodate each of these factors. For example, a pitcher may have particularly good control of a certain pitch and thus favors that pitch, but how can one create a feature to represent its favorability? A potential approach is to create a feature that measures the pitcher's success with a pitch since the beginning of the season, or the previous game, or even the previous batter faced. Which features would best capture the true effect of his preference for that pitch? The answer is that each of these approaches may be best in different situations, so they all must be considered for best accuracy. Pitchers have different dominant pitches, strategies

and experiences; in order to maximize accuracy, our model must be adaptable to various pitching situations. It is noted that in feature space, pitches of same pitch type from different pitchers look different, so classifiers must be trained on each pitcher separately.

Of course, simply adding many features to our model is not necessarily favorable due to the curse of dimensionality. In addition, some features might not be relevant to pitch prediction. Our approach is to change the problem of predicting a pitch into predicting a pitch for each pitcher in a given count. Count, which gives the number of balls and strikes in an at-bat situation, has a significant effect on the pitcher/batter relationship. For example, study by [35] showed that average slugging percentage (a weighted measure of on-base frequency of a batter) is significantly lower in counts that favor the pitcher; however, for neutral counts or counts that favor the batter, there is no significant difference in average slugging percentage. In addition, [31] concluded that pitchers are much more predictable when there are more balls than strikes. These studies show that count is an important factor in making pitch predictions. In order to maximize accuracy, we take an additional step by choosing a most relevant pool of features from the entire available set for each pitcher/count pair. This allows us to maintain our adaptive strategy while controlling dimensionality.

An example of this strategy is shown in Figure 4.1, where we present the selection of predictive features from group 1 for the MLB pitcher Miguel Batista using the data from the 2008 and 2009 seasons when he played for the Seattle Mariners. This figure is segmented by pitching scenarios including batter-favored count, neutral count, and pitcher-favored count. Note that the batter-favored and pitcher-favored counts tend to result in dissimilar feature sets being selected, whereas the neutral counts tend to result in a mixture thereof. More specifically, feature number 6 (lifetime percentage of fastballs thrown) is highly indicative of the *status quo* or standard pitching, it is selected for almost every count except the batter-favored counts (i.e., 3-0, 3-1, 2-0,1-0), where it is selected only once out of 4 counts (pitch count, 1-0). This shows that our feature selection model adapts to the game situation. The pitcher behaves nominally until he is in an unfavorable count, when he often changes his behavior and a priori value of fastball is no longer selected to use in prediction. We also apply this analysis to the other 5 groups of features. It is noted that each count situation yields a different set of features. There are certainly overlapping features, but there is no unique set of features that are chosen in all counts.

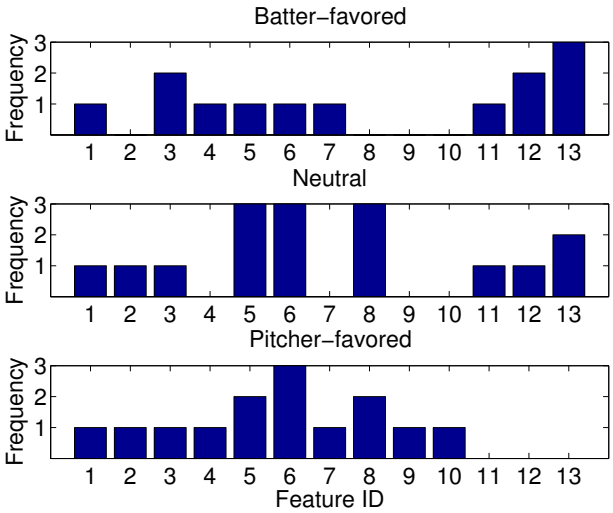

Figure 4.1: Distribution of Group 1 features (1-13) via feature selection method of Miguel Batista (2008-2009).

4.3.2 Model Implementation

As discussed above, our feature selection algorithm is adaptive; that is, we seek a good set of features for each pitcher/count situation. The implementation of this adaptive strategy mainly consists of the following three steps. These steps in our adaptive feature selection approach are summarized and depicted in Figure 4.2.

1. Select a subset of features (18) from the raw data and create additional features (59) from the data that are deemed more relevant to pitch prediction. This set of 77 features is further divided into 6 groups of similar features. The number of features from each group varies from 6 to 22 (see the full list in the Appendix A.1).

2. Compute the receiver operating characteristic (ROC) curve and the corresponding area under curve (AUC) for each group of features, then select the most useful features for pitch prediction. In practice, selecting only the best feature provides worse prediction than selecting the best two or three. Hence, at this stage, the size of each group is reduced from 6-22 features to 1-10.

3. Remove all redundant features from our final set. From our grouping, features are

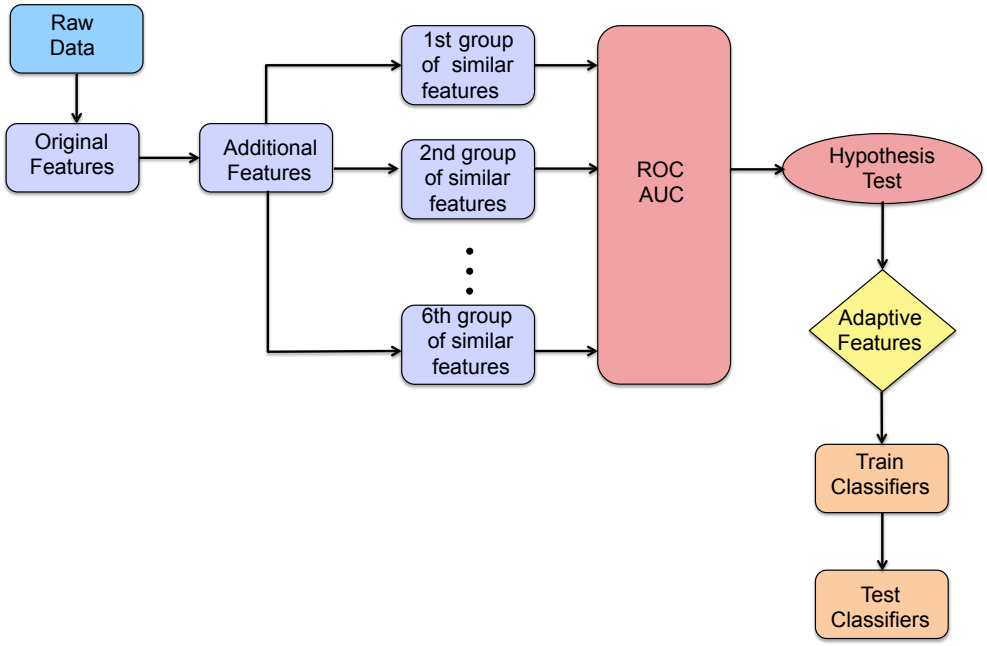

Figure 4.2: Schematic diagram of the proposed adaptive feature selection.

taken based on their relative strength. There is the possibility that a group of features may have poor predictive power. In those instances, we want to prune them from our feature set before we begin to predict. The resulting set of features is pruned by conducting a hypothesis testing to measure the significance of each feature at the $\alpha = .01$ level.

4.3.3 ROC Curves

Receiver operating characteristic (ROC) curves are two-dimensional graphs that are commonly used to visualize and select classifiers based on their performance [30]. They have been used in many applications including signal detection theory [28] and diagnostic tools in clinical medicine [56, 72]. It is noted that a common method to determine the performance of classifiers is to calculate the area under the ROC curve, often denoted by AUC [13]. An example of a ROC curve using data from PITCHf/x pitch tracking system is depicted in Figure 4.3.

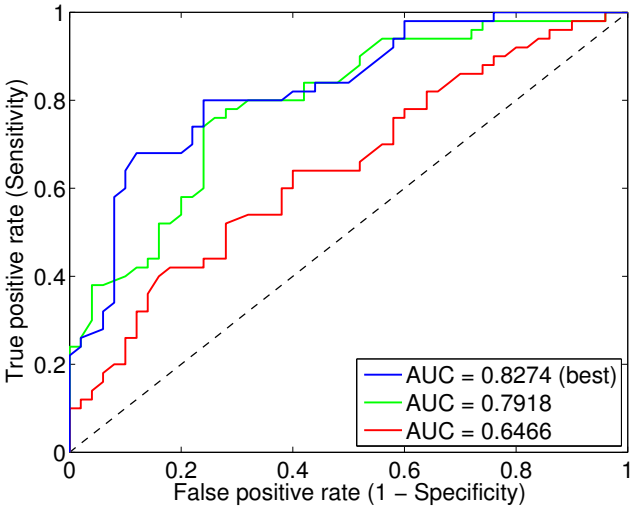

Figure 4.3: ROC curve. In this example, three features are measured with the ROC curve. The blue curve represents the best feature among the three since it has the highest AUC. The diagonal line represents random guessing. The area between a ROC curve and the diagonal line quantifies how much better that feature is at distinguishing the two classes compared to random guessing.

4.3.4 Hypothesis Testing

The ability of a feature to distinguish between two classes can be verified by using a hypothesis test. Given any feature f, we compare μ_1 and μ_2, the mean values of f in Class 1 (*fastballs*) and Class 2 (*nonfastballs*), respectively. Then we consider

$$H_0 : \mu_1 = \mu_2$$
$$H_A : \mu_1 \neq \mu_2$$

and conduct a hypothesis test based on the student's t distribution. We compare the p-value of the test against a significance level of $\alpha = .01$. When the p-value is less than α, we

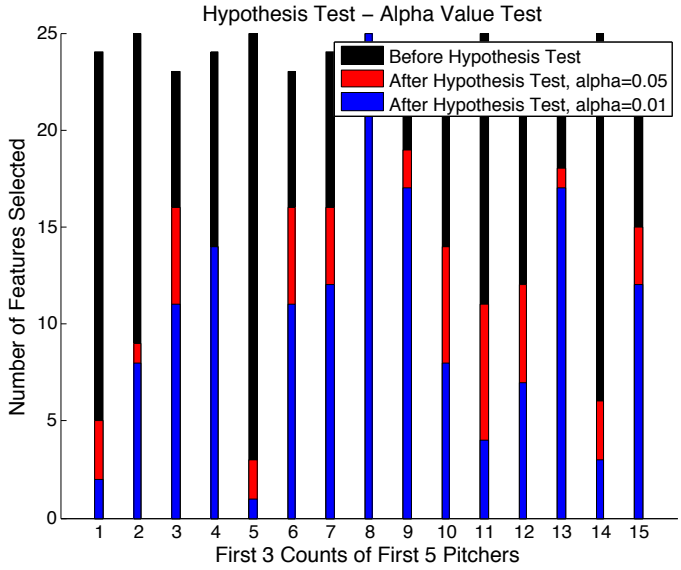

Figure 4.4: Hypotheis testing for feature selection. The black bars are the number of features returned by the ROC curve test, the blue are the features considered optimal for $\alpha = .01$, the red are for $\alpha = 0.05$.

reject the null hypothesis and conclude that the studied feature means are different for each class, meaning that the feature is significant in separating the classes. In that sense,

this test allows us to remove features which have insignificant separation power.

Figure 4.4 depicts the hypothesis testing step for the first 15 pitcher-count pairs in our dataset. The number of features rise in the optimal set when we increase $\alpha = .01$ to $\alpha = .05$ as expected. In our experiment, the accuracy, however, is lowered than the stricter significant level. It is also important to notice that the number of the optimal features is varying throughout different pitcher-count pairs.

4.3.5 Classification

Classification is the process of taking an unlabeled data observation and using some rule or decision making process to assign a label to it as presented earlier in Chapter 2. Within the scope of this study, classification represents determining the type of a pitch, i.e., given a pitch x with characteristics x_i, determine the pitch type x is. Several classification can be used to accomplish this task. The methods used in this study are the k-nearest neighbor (k-NN), the Linear Discriminant Analysis (LDA) and the Support Vector Machine (SVM), see chapter 2 for a discussion of each method.

4.4 Results Analysis

To form a baseline for our prediction results, the prediction model is compared against the naive guess model. The naive guess simply returns the most frequent pitch type thrown by each pitcher, calculated from the training set, see [31]. The improvement factor I is calculated as follows:

$$I = \frac{A_1 - A_0}{A_0} \times 100 \tag{4.1}$$

where A_0 and A_1 denotes the accuracies of naive guess and our model, respectively.

4.4.1 Overall Results

We apply prediction techniques to all pitchers who threw at least 750 pitches in both 2008 and 2009. After performing feature selection on each data subset, each classifier (see Appendix A.3) is trained on data from 2008 and tested on data from 2009. The average classification accuracy for each classifier is computed for test points with a type confidence

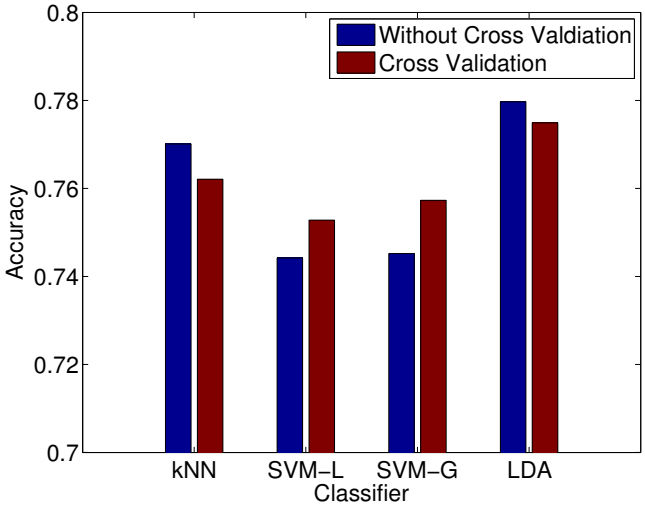

Figure 4.5: Prediction accuracy comparison (percents). Symbol: k-Nearest Neighbors (k-NN), Support Vector Machine with linear kernel (SVM-L), and with Gaussian kernel (SVM-G), Linear Discriminant Analysis (LDA), Prediction Tree (PT).

of at least 90%. Type confidence, one of the original features from raw data (see Table 4.1), estimates the accuracy of the class labeling by PITCHf/x, that is, how confidence can we assure that a pitch label (pitch type) is correctly determined.

Figure 4.5 depicts the average accuracies among all applicable pitches in 2009 season. LDA outperforms the other methods at 78% on average accuracy, k-NN comes closely in second at 77%. Compared to the naive model's prediction accuracy, our model yields a 21% improvement. In previous work, the average prediction accuracy of the 2009 season is 70% with 18% improvement [31]. It should be noted that previous work uses the linear SVM classifier and considers 359 pitchers who threw at least 300 pitches in both the 2008 and 2009 seasons.

In addition, with cross validation implemented, our accuracies remain stable within ±2% of the original results. This serves as an important confirmation that our results are reliable and our methods would perform well when applied to a newly introduced data set.

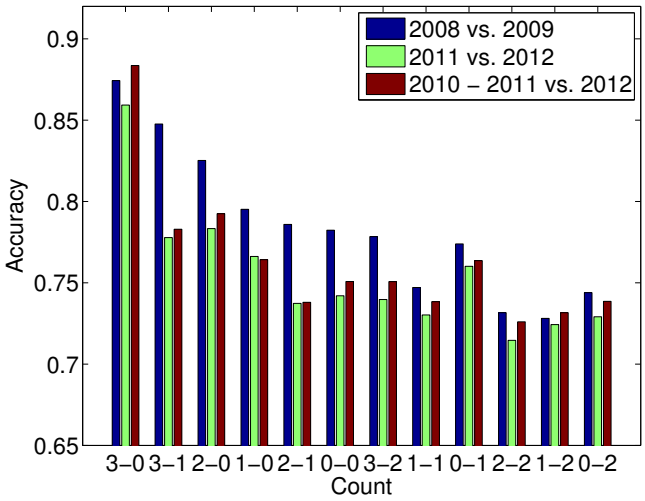

Figure 4.6: Prediction accuracy by count.

4.4.2 By Count Analysis

Figure 4.6 depicts average prediction accuracy per each count situation. Accuracy is significantly higher in batter favored counts and approximately equal in neutral and pitcher favored counts. Prediction is best at the 3-0 count (89%) and worst at the 1-2 and 2-2 counts (73%). In addition, we also calculate prediction accuracy for the 2012 season, using training data from the 2011 season or from both the 2010 and 2011 seasons, shown in Figure 4.6. Even though the size of training data is double in the latter case, we only gain very minimal prediction accuracies at every count situation.

4.4.3 By Pitcher Analysis

We also selected eight pitchers from the 2008 and 2009 MLB regular seasons to examine in details with SVM and k-NN classifiers.

Table 4.2 describes the training and testing sets. Data from 2008 season were used for training and data from 2009 were used for testing. Table 4.3 depicts the prediction accuracy among the eight pitchers as compared across SVM and k-NN classifiers as well as naive guess. On average, 79.76% of pitches are correctly predicted by SVM-L and SVM-G classifiers

Table 4.2: Data for each pitcher.

Pitcher	Training Size	Test Size
Fuentes	919	798
Madson	975	958
Meche	2821	1822
Park	1309	1178
Rivera	797	850
Vaquez	2412	2721
Wakefield	2110	1573
Weathers	943	813

Table 4.3: Prediction accuracy comparison (percents). Symbols: k-Nearest Neighbors (k-NN), Support Vector Machine with linear kernel (SVM-L), Support Vector Machine with Gaussian kernel (SVM-G), Naive Guess (NG).

Pitcher	k-NN	SVM-L	SVM-G	NG
Fuentes	80.15	78.38	76.74	71.05
Madson	81.85	77.23	79.38	25.56
Meche	72.73	74.83	74.17	50.77
Park	70.31	72.40	71.88	52.60
Rivera	93.51	89.44	90.14	89.63
Vaquez	72.50	72.50	73.05	51.20
Wakefield	100.00	95.50	96.33	100.00
Weathers	76.01	77.76	76.38	35.55
Average	80.88	79.76	79.76	66.04

while k-NN perform slightly better, at 80.88% accurate. Furthermore, k-NN is also a better choice in term of computational speed, as noted in Table 4.4. Table 4.5 presents the best

Table 4.4: CPU Times (seconds)

Pitcher	k-NN	SVM-L	SVM-G
Fuentes	0.3459	0.7357	0.3952
Madson	0.3479	0.5840	0.4076
Meche	0.3927	1.2616	0.7270
Park	0.3566	0.7322	0.4591
Rivera	0.4245	0.6441	0.4594
Vaquez	0.4137	1.1282	0.7248
Wakefield	0.4060	0.3057	0.5267
Weathers	0.3480	0.5315	0.3641
Average	0.3794	0.7408	0.5799

Table 4.5: Best Improvement over Naive Guess (percents)

Pitcher	Improvement	Classifier
Fuentes	12.81	k-NN
Madson	22.01	k-NN
Meche	47.39	SVM-L
Park	37.62	SVM-L
Rivera	0.04	k-NN
Vaquez	42.68	SVM-G
Wakefield	0.00	k-NN
Weathers	118.73	SVM-L

classifier that yields highest improvement over Naive guess. In fact, different classifiers perform differently among pitchers.

4.4.4 By Noise Level

PITCHf/x provide a type confidence value associated with every pitch being recorded, which indicates the likelihood of a pitch type being correctly classified. Intuitively, it measures the quality of our data and one can think of instances with low type confidence as having high level of noise. Of course we want to build our prediction algorithm in the noiseless environment. However, as shown in Table 4.6, higher the type confidence cut off thresholds reduce the sizes of testing sets. In fact, majority of test points have an 80% or higher type confidence (lower noise). There is not a significant reduction in test sizes from the

Table 4.6: Prediction results by Type Confidence levels (TC). Symbol: k-Nearest Neighbors (k-NN), Support Vector Machine with linear kernel (SVM-L), and with Gaussian kernel (SVM-G), Linear Discriminant Analysis (LDA).

TC (%)	50	60	70	80	90	95	99
Test size	355,755	344,300	332,238	312,574	196,853	24,412	7,150
k-NN	75.94	75.58	75.88	75.72	77.01	84.49	84.63
SVM-L	73.99	73.99	73.99	74.05	74.42	77.00	73.94
SVM-G	74.02	74.03	74.07	74.16	74.52	76.02	72.07
LDA	77.19	77.17	77.13	77.13	77.97	83.19	81.76

50% level (355,755) to the 80% level (312,574), hence prediction performances from all methods remain stable throughout these intervals. Only when the cut-off threshold of type confidence is raised to 90% level, we can notice the reduction in test sizes and the increasing in average prediction accuracies among all methods. We obtain even higher average prediction accuracies at the 95% level where LDA is 83% and k-NN is 84% accurate. However, there are only $24,412$ pitches at this level, less than 7% of all pitches from original test set of about $360,000$ pitches, at the 0% level. Hence, we choose the 90% level to be the most reasonable choice to cut off, which contains more than 50% of the original test points. Notice that even at a low type confidence level of 50%, LDA still outperforms other methods, resulting in 78% accuracy. Unlike LDA and k-NN, SVM based classifiers show only minimal improvement when noisy data are removed. Originally, SVM classifier was built to reduce the impact of noise and to enhance generality in classification (we have shown that the

SVM has Tikhonov regularization embedded in section 3.1). Furthermore, only the support vectors (a subset of training data) are used in the final decision function while the rest of the training data are not considered (section 2.3). It would be very likely that those data points with low level of type confidence are not selected to be support vectors. Thus, SVM results are consistency among different levels of type confidence threshold cut-off. This is indeed the motivation for us to focus on implement SVM based classifier for our medical diagnosis work where the datasets are much smaller and the presence of noise is not negligible.

CHAPTER

5

MEDICAL DIAGNOSIS

Medical diagnostic decision support systems (MDSS) play important role in assisting physicians with making clinical decisions. Berner et al. (1999) suggest that physicians' performance can be strongly influenced by the quality of the information the system [1] produce and the type of cases on which the system is used. Physicians' diagnostic performance is significant higher on easier cases for which MDSS could provide higher-quality information [46]. The less than ideal performance on harder cases motivates researchers to seek for better diagnostic models because the cost of *false negative* [2] is often too high in health care.

[1] In this research, a national sample of 67 internists, 35 family physicians, and 6 other physicians use Quick Medical Reference diagnostic support system to assist them in the diagnosis of clinical case. Three sets of eight cases, stratified by diagnostic difficulty and the potential of QMR to produce high-quality information, were used. The effects of using QMR on three measures of physicians diagnostic performance were analyzed using analyses of variance [46].

[2] False negative refers to incorrectly indicating a person does not have a disease or condition when the person actually does have it.

5.1 Previous Work

Machine learning applied to medical diagnosis has become an incredibly active field of research. Many techniques for classification of hepatitis disease diagnosis [2–4, 21, 26, 40, 47, 71] and breast cancer [5, 24, 39, 41, 52, 54, 64, 66, 67] have been presented in the literature. Regarding hepatitis C diagnosis, it can be seen in Table 5.1 that various classification methods are used including both nonparametric and parametric classifiers. Nonparametric methods in this list are the Multilayer Perceptron (MLP), the Generalized Regression Neural Network (GRNN), the Principal Component Analysis-Artificial Neural Network (PCA-ANN), the k-nearest neighbor (k-NN) and the weighted k-NN. Meanwhile, the Radial Basis Function (RBF), the Linear Discriminant Analysis (LDA), the Quadratic Discriminant Analysis (LDA) and the Support Vector Machine (SVM) are parametric models.

Few researchers experiment with both types and often parametric classifiers yield better accuracy. For example, Ozyildirim obtains 83.75 % with RBF, 80 % with GRNN and 74.37% with MLP. Ster and Dobnikar obtain 85.8 % and 86.4% with LDA and QDA respectively as compared to 85.3 % non parametric 1-NN. The Artificial Neural Network classifier with the addition of dimension reduction technique Principal Component Analysis (PCA-ANN) reached 89.6%.

The two most recent results, also with highest accuracies, are based on the Support Vector Machine. Chen Liu et al (2011) propose a hybrid method based on Local Fisher Discriminant Analysis and Support Vector Machine (LFDA-SVM). LFDA reduces the original 19 feature set to 2 feature subset when pair with SVM, obtains 96.77 % accuracy [21]. Afif et al on the other hand utilize scatter search to find the optimal tradeoff constant C for the SVM, results in 98.75% accuracy [4]. These notable results motivate us to build our model around SVM classifier.

These two SVM approaches require parameters optimization. The LFDA-SVM uses grid search to find optimal values for tradeoff constant C and Gaussian kernel parameter γ while the SS-SVM optimized only C with the scatter search method (it is unclear which kernel function was used in Afif's study). We adopt the important idea of parameters optimization and also use grid search to find the best C and γ. However, we pay more emphasis on avoiding *overfitting* possibility because of the imbalanced dataset. To do so, we

(1) introduce different balanced evaluation metrics pair within the parameters optimization procedure and (2) construct a modified weighted cost function that is sensitive to the ratio of the numbers of positive and negative instances in the dataset. For more details, see section 5.3.3 and 5.3.2, respectively.

Regarding breast cancer diagnosis, as seen in Table 5.2, very similar techniques are conducted. In fact, Ster and Dobnikar, Polate and Gunes apply the same method on both hepatitis C and breast cancer datasets and get comparable results. It's also worth mentioning that similar to hepatitis C, the two most recent and best performed methods in breast cancer diagnosis are also SVM based.

Table 5.1: Hepatitis C classification accuracies comparison among recent studies.

Author	Method	Validation	Year	Accuracy (%)
Ster and Dobnikar	1-NN	10-fold CV	1996	85.30
Ster and Dobnikar	QDA	10-fold CV	1996	85.80
Ster and Dobnikar	LDA	10-fold CV	1996	86.40
Grudzinski	15NN,stand.Euclidean	10-fold CV	1998	89.00
Grudzinski	18NN,stand.Manhattan	10-fold CV	1998	90.20
Grudzinski	Weighted 9-NN	10-fold CV	1998	92.90
Ozyildirim, Yildirim	MLP[3]	5-fold CV	2003	74.37
Ozyildirim, Yildirim	GRNN[4]	5-fold CV	2003	80.0
Ozyildirim, Yildirim	RBF[5]	5-fold CV	2003	83.75
Polat and Gunes	PCA-AIRS[6]	10-fold CV	2007	94.12
Dogantekin, Avci, et al.	LDA-ANFIS[7]	10-fold CV	2007	94.16
Jilani, Tahseen et al	PCA-ANN[8]	70-30% hold-out	2009	89.60
Chen,Liu, et al	LFDA-SVM[9]	80-20% hold-out	2011	96.77
Afif, Mohamed et al	SS-SVM[10]	10-fold CV	2013	98.75

[3]MLP: Multi-layer Perceptrons
[4]GRNN: Generalized regression neural network
[5]RBF: Radial Basis Function
[7]PCA-ANN: Principal Component Analysis-Artificial Neural Network
[6]PCA-AIRS: Principal Component Analysis- Artificial Immune Recognition System
[8]LDA-ANFIS: Linear Discriminant Analysis- Adaptive Network Based Fuzzy Inference System
[9]LFDA-SVM: Linear Fisher Discriminant Analysis-Support Vector Machine
[10]SS-SVM: Scatter Search- Support Vector Machine

Table 5.2: Breast cancer classification accuracies comparison among recent studies.

Author	Method	Validation	Year	Accuracy (%)
Quinlan	C4.5	10-fold CV	1996	94.74
Hamiton et al.	RIAC	10-fold CV	1996	95.00
Ster and Dobnika	LDA	10-fold CV	1996	96.80
Bennett and Blue	SVM	5-fold CV	1997	97.20
Nauck and Kruse	NEFCLASS	10-fold CV	1999	95.06
Pena-Reyes and Sipper	Fuzzy-GA1	75-25 % hold-out	1999	97.36
Setiono	Neuro-rule 2a	50-50% hold-out	2000	98.10
Goodman et al.	Optimized-LVQ	10-fold CV	2002	96.70
Goodman et al.	Big LVQ	10-fold CV	2002	96.80
Goodman et al.	AIRS	10-fold CV	2002	97.20
Albrecht et al.	LSA with Perceptron	10-fold CV	2002	98.80
Abonyi and Szeifert	Supervised fuzzy clustering	10-fold CV	2003	95.57
Polat and Gunes	Fuzzy-AIS-kNN	10-fold CV	2005	95.57
Polat and Gunes	LS-SVM	10-fold CV	2007	98.53
Akay, Mehmet	FS-SVM	80-20% hold-out	2009	99.51

5.2 Class Imbalance and Related Work

In our initial attempt, we run various classifiers on the Hepatitis C dataset such as the k-NN ($k = 5, 9, 15$), LDA, SVM-L and SVM-G (directly without modification and parameters tuning). To our surprise, without much effort, the results happen to be fairly good, comparable to the first 5 studies in Table 5.1. For each classifier, we then repeat the learning process 500 times with 10-fold CV at each repetition. As depicted in Figure 5.1, consider the median performance, most classifiers reach over 80% accuracy. The worst performance is 5-NN, at about 78% accuracy. It is also the worst in term of variability, where its performance ranges from 73% to 84%. On the other hand, the SVM-L and the SVM-G are the best two classifiers, obtain 86% and 84% accuracy, respectively. These two classifiers, however, come with noticeably high variability. The most stable classifier is 15-NN which constantly achieves 80% accuracy in almost every repetition. At this point, if we have only one choice for selecting a classifier then the 15-NN is indeed the best candidate because of its low variability (recall the context of estimation E_{out} via E_{val} in section 3.2.2). However, looking

further, we realize that the15-NN assigns all observation to the negative (majority) class in both training and validation set. In fact, the accuracy that the 15-NN obtains, 80% equals to the percentage of negative observations in the Hepatitis C dataset which contains 123 negative and 32 positive observations (full description of the dataset is presented in Table 5.3). To the lesser extent, other classifiers such as LDA and SVM-L and SVM-G also suffer

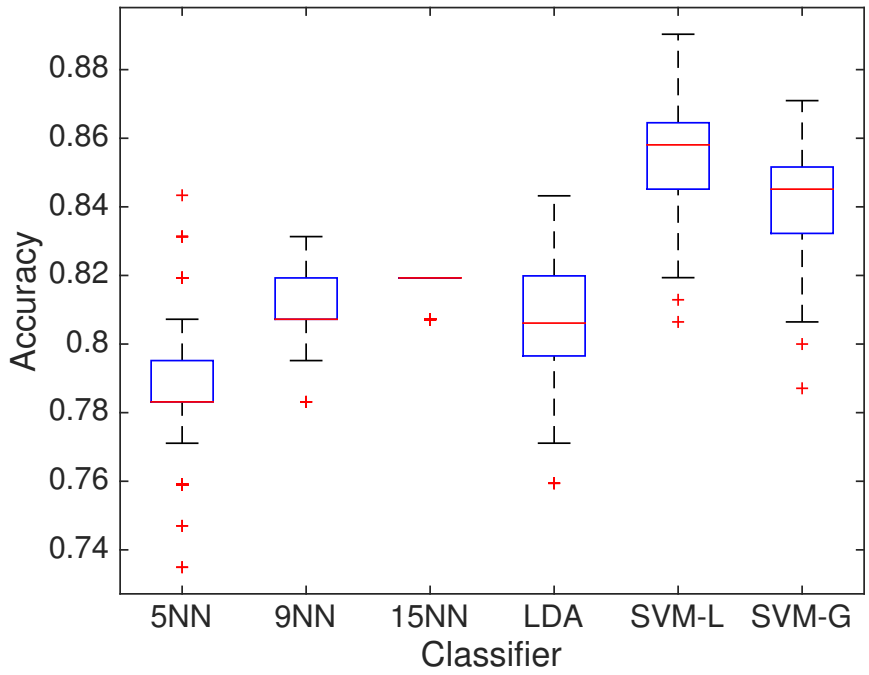

Figure 5.1: Hepatitis C classification comparison with 10-fold CV over $N = 500$ repetitions.

by the class imbalance, resulting in its inability to correctly classify the observations of the positive (minority) class. The extreme case of 15-NN can be seen as an underfitting problem, where the final hypothesis is much simpler than the target function. Overall, this can be considered as an overfitting problem because the learning hypothesis although appears to (over)fit the data nearly perfectly (in term of accuracy), it obviously cannot be trusted in predicting future (unseen) observation, especially in detecting positive instances.

Besides medical diagnosis, class imbalance is very popular in other application domains

such as gene profiling, (email) spam detection and credit card fraud detection. For example, an imbalance of 100 to 1 exists in fraud detection [53]. Classifiers perform poorly on unbalanced datasets because they are often designed to output the simplest hypothesis that best fits the data. For example, recall the soft-margin SVM (section 2.3.2) which can be seen as an Tikhonov regularization (section 3.1) to reduce model complexity. This approach works well on balanced dataset (pitch prediction in previous chapter) but it often fails with highly unbalanced datasets where the simplest model is often the one that classifies every instance as negative. Thus, the classifiers consider positive instances as noise and ignore them in the learning process.

Previous work on class imbalance classification can be categorized into two main divisions: the data processing approach and the algorithmic approach [7, 34, 69].The data processing approach is to adjust the class distribution of the data set by either under-sampling the majority class or over-sampling the minority class. An example of under-sampling, presented in [42, 43], is to remove noisy and redundant majority instances. This method can be challenging to use for small datasets (such as our Hepatitis C) where removing data points can be expensive. Over-sampling is the opposite of under-sampling approach. Authors in [20] suggest duplicating and/or interpolating minority instances under the method called SMOTE [11]. SMOTE assumes the neighborhood of a positive instance to be positive and instances that locate between two positive instances are also positive. These assumptions may not be true and can be data-dependent so again with small datasets, it would raise the problem of inconsistency. For example, with cross validation, at each iteration, a different partition of training and validation sets is formed, hence the idea of positive neighborhood or the space between two positive instances may fail to remain intact. Furthermore, both under-sampling and over-sampling techniques attempt to change the class distribution, in turn, change class prior. Hence, it violates the assumption of many Bayesian classifiers, such as LDA classifier where the discriminant function uses the estimate of the prior probability that a random chosen observation is associated with a certain class (section 2.2) [70]. Although the SVM is not directly affected by adjusting class prior, the inconsistency performance with small datasets is enough for us to skip the under-sampling and over-sampling techniques in our model.

[11] SMOTE: Synthetic Minority Oversampling Technique

The algorithmic approach, which is adopted in our study, is to bias the classifiers so that they pay more attention to the positive instances. In the SVM regime, this is equivalent to assign higher cost in misclassifying positive instances (we will discuss this further in section 5.3.2). This idea is first suggested by Veropoulos et al [61] and its later extensions can be found in [15, 45, 63]. Algorithmic approach also applies to other classifiers such as [49] on modified multilayer perceptron or [25, 29] decision tree generator.

5.3 Model Implementation

Our benchmark is the study of Akbani et al [7]. The authors apply SVM with Veropoulos's cost sensitive approach [61] and implement SMOTE [20] in attempt to combat class imbalance. Their model is tested with 10-fold cross validation on many unbalanced data sets, including the UCI Hepatitis C dataset we use here. For our study, we employ the cost sensitive approach (of using different penalty constants for different classes) combing with Gaussian kernel parameter optimization on soft margin SVM. The steps of our diagnosis model is depicted in Figure 5.2. Our model is implemented in the LIBSVM package for MATLAB. LIBSVM software and its documentation can be found in [19].

5.3.1 Data Preprocessing

We perform our experiments on the Hepatitis C dataset taken from the UCI machine learning repository [44]. The dataset contains 155 observations, of which 32 of them are labeled *die* while the remaining 123 observations are labeled *live*. Beside class label, 19 features are associated with each observation from which 13 are binary values and 6 contains discrete values. The description of all features in this dataset is presented in Table 5.3.

The data preparation process prior applying the SVM involves transforming categorical feature to vector and scaling. The SVM requires that each instance is represented as a vector of real numbers. To do this, we adapt the converting procedure suggested in [36], a vector of length m is used to represent an m-category attribute. Only one of the m numbers is one, and the others are zero. For example, a three-category attribute {red, green, blue} will be represented as $(0,0,1),(0,1,0)$, and $(1,0,0)$ instead of using a single indicator number such as 1,2, and 3 [36].

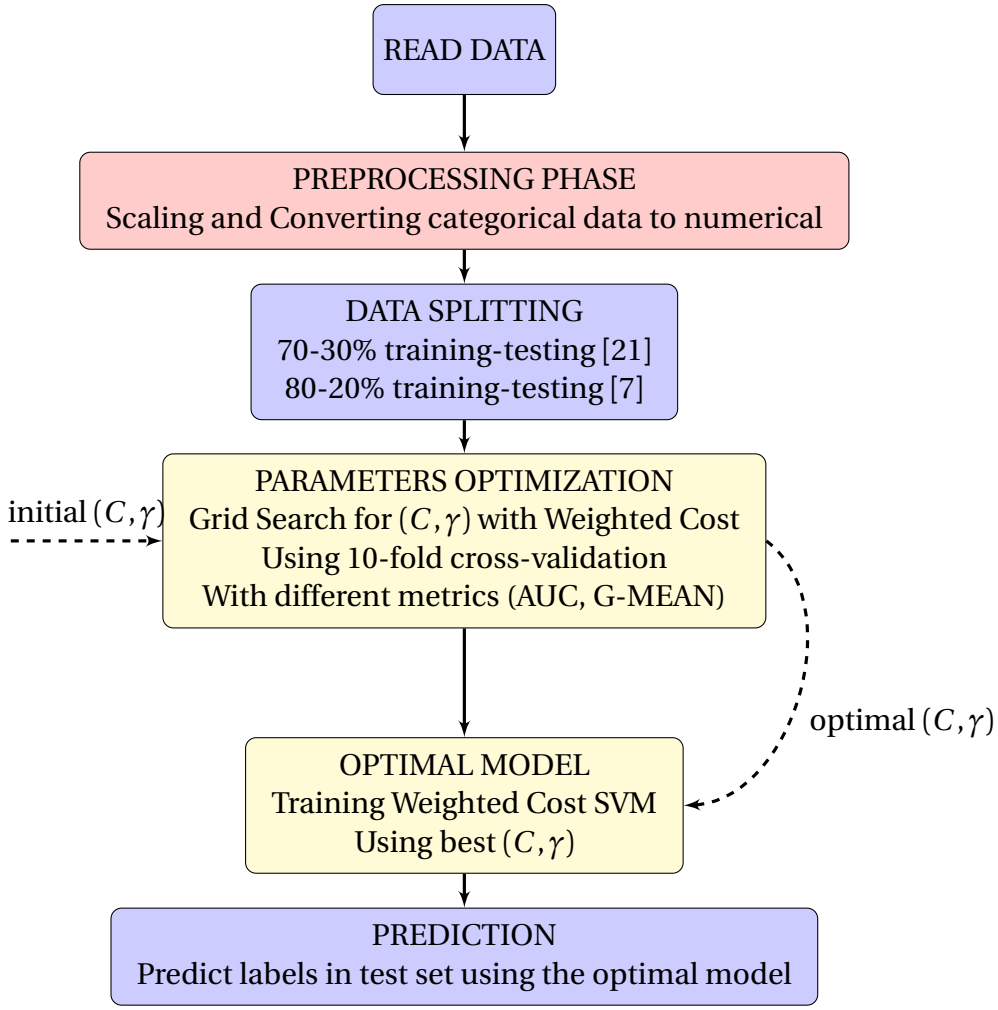

Figure 5.2: Schematic diagram of the proposed diagnosis classification

Table 5.3: Hepatitis C data: description of attributes. See Appendix B.1 for the definitions of some of the attributes.

No	Variable	Values	# of Missings
1	Class	Die (32), Alive (123)	0
2	AGE	7-78	0
3	SEX	Male, Female	0
4	STEROID	Yes, No	1
5	ANTIVIRALS	Yes, No	0
6	FATIGUE	Yes, No	1
7	MALAISE	Yes, No	1
8	ANOREXIA	Yes, No	1
9	LIVER BIG	Yes, No	10
10	LIVER FIRM	Yes, No	11
11	SPLEEN PALPABLE	Yes, No	5
12	SPIDERS	Yes, No	5
13	ASCITES	Yes, No	5
14	VARICES	Yes, No	5
15	BILIRUBIN	0.39- 4.0	6
16	ALK PHOSPHATE	33-250	29
17	SGOT	13-500	4
18	ALBUMIN	2.1-6.0	16
19	PROTIME	10-90	67
20	HISTOLOGY	Yes, No	20

Scaling is another important step before applying the SVM. Its main advantage is to avoid attributes with greater values dominating smaller ones. Another advantage of scaling is to avoid numerical difficulties during kernel calculations because kernel values depend on the inner product of features vector, as pointed out in [18, 36]. In our experiment, we linearly scale each attribute to the range $[-1,1]$ for both training and testing datasets. We use the following equation to convert a value $x \in [a,b]$ to $\bar{x} \in [-1,1]$:

$$\bar{x} = \frac{2(x-a)}{b-a} - 1.$$

5.3.2 Cost Sensitive SVM

For unbalanced classes, researchers have proposed using different penalty parameters in SVM cost function [18], also referred to as weighted cost SVM. The standard two-class problem SVM (2.53) in section 2.3 becomes

$$\begin{aligned} \min \quad & \frac{1}{2} w^T w + C^+ \sum_{y_i=1} \xi_i + C^- \sum_{y_i=-1} \xi_i, \\ \text{subject to} \quad & y_i (w^T \phi(x_i) + b) \geq 1 - \xi_i, \\ & \xi_i \geq 0, i = 1, ..., l, \end{aligned} \tag{5.1}$$

where C^+ and C^- are regularization parameters for positive and negative classes respectively. The dual problem of (5.1) is

$$\begin{aligned} \min \quad & \frac{1}{2} \alpha^T Q \alpha - e^T \alpha, \\ \text{subject to} \quad & 0 \leq \alpha_i \leq C^+, \quad \text{if} \quad y_i = 1, \\ & 0 \leq \alpha_i \leq C^-, \quad \text{if} \quad y_i = -1, \\ & y^T \alpha = 0, \end{aligned} \tag{5.2}$$

where $e = [1, \cdots, 1]^T$ is the vector of all ones, Q is an l by l positive semidefinite matrix $Q_{ij} = y_i y_j K(x_i, x_j)$ and $K(x_i, x_j) = \phi(x_i)^T \phi(x_j)$ is the kernel function. This new constrained optimization problem again can be solved using Lagrangian method as previously mentioned in section 2.3. A detailed explanation of this extension to the standard SVM problem

is presented in [18].

In an extreme case, one can assign each instance x_i a regularization parameter C_i, $i = 1, \cdots, N$. However, this make the cost function *over sensitive* and indeed our classification will be more likely to overfit the training data. In our experiment, weights are calculated simply as follows

$$\frac{C^+}{C^-} = \frac{n^-}{n^+}, \tag{5.3}$$

where n^+ and n^- are number of instances belonging to the positive and negative classes, respectively [12].

5.3.3 Parameters Optimization

In addition to data processing, proper model parameters setting plays an important role in the SVM performance. When using kernel tricks for the SVM, there are parameters that need to be chosen in advance: (1) the regularization parameter C which is the tradeoff cost between minimizing classification error and maximizing the margin (in fact, tuning C can be viewed as a way to control overfitting [60]); (2) the choice of kernel functions to be used in the SVM which defines the mapping from the input space to some high dimensional feature space; and (3) the kernel parameters [57, 60]. The polynomial kernel has more hyperparameters to adjust than the Gaussian kernel, they may in fact even go to infinity or zero if the degree is large. Meanwhile, Gaussian kernel has only one parameter γ. We implement the grid search technique, also called parameter sweep, with 10-fold cross validation to find the optimal parameter value of the pair (C, γ) [36]. The grid search procedure is as follows,

1. consider a grid space of (C, γ) with $\log_2 C \in \{-5, -3, \cdots, 15\}$ and $\log_2 \gamma \in \{-15, -13, \cdots, 3\}$,
2. for each pair (C, γ) in the search space, perform 10-fold CV on the training set,
3. choose the parameter (C, γ) that yields the lowest error rate under balanced metrics,
4. use the optimal parameters to create a SVM model as the predictor.

[12] In this chapter, positive denotes minority class while negative denotes the majority class.

Previously, researchers who use SVM either take accuracy at this step instead and only employ certain balanced evaluation metric at the end to assess the final predictor model [4, 7, 21]. To emphasize the treatment to overfitting caused by class imbalance, we replace accuracy by other class balanced evaluation metrics including G-mean, AUC (see section 5.3.4) in step 3 of the above procedure, and chose the pair (C,γ) that yields the lowest average error associated with each evaluation metric, respectively.

Our grid search result on Hepatitis C data is shown in Figure 5.3. The two parameters C and γ are displayed in logarithmic axes x and y. The lines indicate areas of the grid searches. The colors of the lines indicate the quality of the solutions.

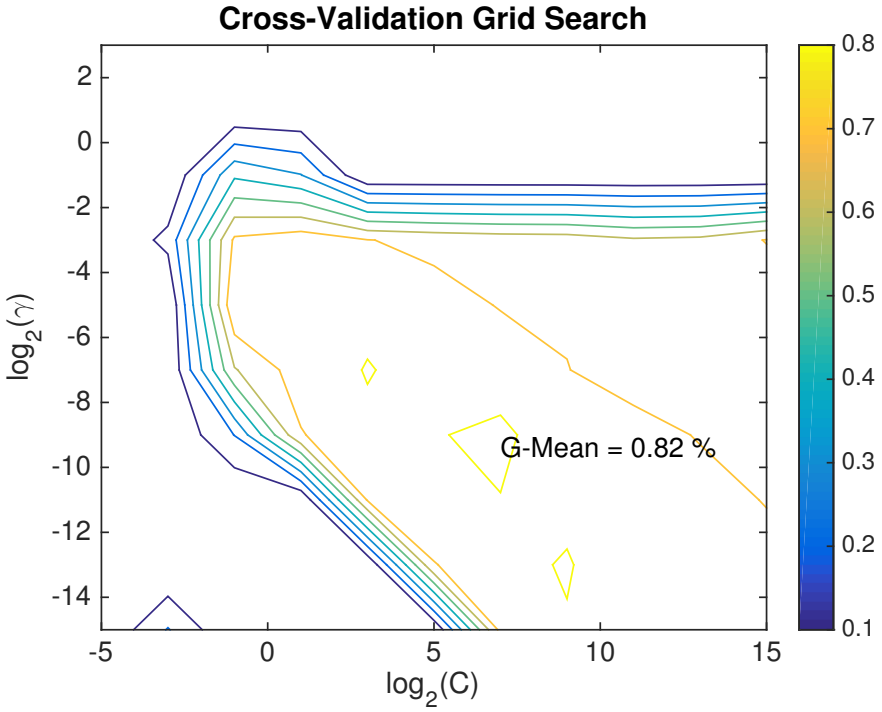

Figure 5.3: Parameter Optimization via Grid Search on Hepatitis C (10-CV).

5.3.4 Evaluation Metrics

Accuracy is a poor choice for model evaluation on unbalanced datasets as seen in previously. The machine learning and medical communities mainly use two metrics, sensitivity and specificity to evaluate the model performance [7]. Sensitivity, also called recall or true positive rate, is defined as the accuracy on the positive instances,

$$\text{Sensitivity} = \frac{\text{True Positive}}{\text{True Positive} + \text{False Negative}} = \text{Recall},$$

while specificity is defined as the accuracy on the negative instances,

$$\text{Specificity} = \frac{\text{True Negative}}{\text{True Negative} + \text{False Positive}}.$$

There is a variety of ways to combine sensitivity and specificity into a single metric. Kubat et al [42] suggest the G-Means metric defined

$$g = \sqrt{\text{Sensitivity} \times \text{Specificity}}$$

This metric is used by authors from our benchmark study [7] and several researchers in the references there of, [42, 43, 69]. We use G-mean and also list sensitivity and specificity separately in the evaluation of our classifier so that the results can be easily compared. In addition, we also employ ROC-AUC metric in our evaluation, ROC-AUC is previously introduced in section 4.3.3.

5.4 Results Analysis

In our experiments of the Hepatitis C classification, we first compare our classifier with the regular SVM-L (SVM using linear kernel), the regular SVM-G (SVM using Gaussian kernel), the SVM-G with Grid Search, the SVM-L with Weighted Cost, the SVM-G with Weighted Cost, and finally the SVM-G with Weighted Cost and Grid Search. These classifiers are sorted in the order of algorithmic complexity in Figure 5.4. Typically small datasets result in higher variability in testing due to the nature of training-testing partitioning (section

3.2). To address this challenge, we run the tests 500 times and take the median result as the safe way to compare classifiers performance. The results of these experiments using G-Mean and ROC-AUC metrics are given below

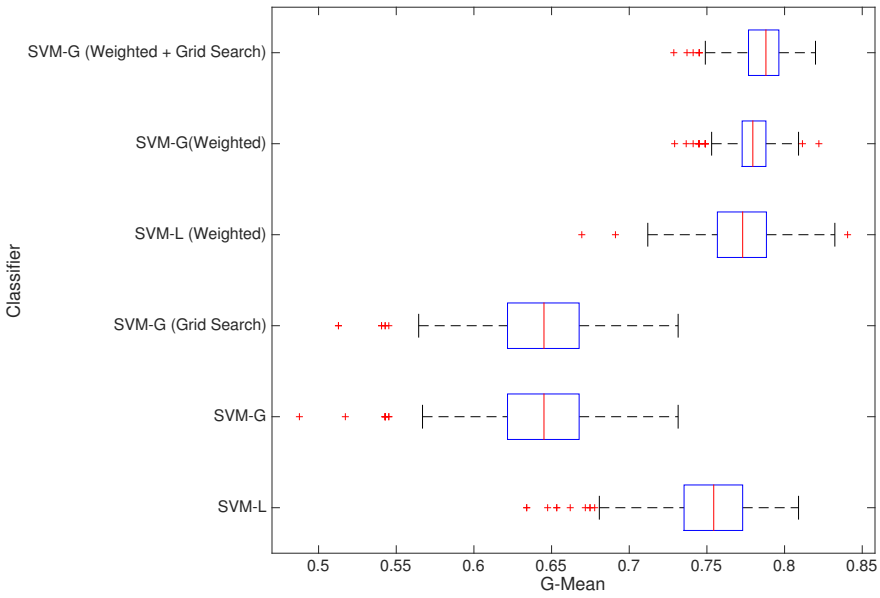

Figure 5.4: G-Mean comparison on Hepatitis C dataset with 10-fold CV over $N = 500$ repetitions.

As shown in Figures 5.4 5.5, the results from both metrics are almost identical. The regular SVM-G and the SVM-G with Grid Search are the worst performer and has highest (bad) variability. Next come the regular SVM-L and the SVM-L with Weighted Cost even though they both have high variances as well. Overall, in both G-Mean and AUC metrics, the SVM-G with Weighted Cost and Grid Search is the best classifier, measured in median results. In term of variability, however the SVM-G with Weighted Cost performs best (lowest variance) in G-Mean metric. The two classifiers tie in ROC-AUC metric regarding consistency. We realize that a different training-test set are chosen at each run yields different pairs of optimal (C, γ) with Grid Search. Hence, it would very likely be the cause of slightly higher

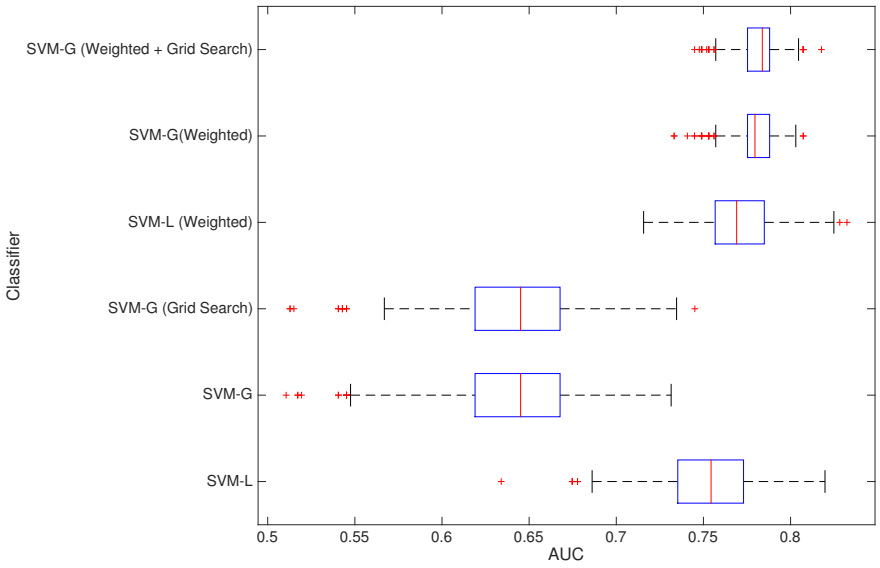

Figure 5.5: ROC-AUC comparison on Hepatitis C dataset with 10-fold CV over $N = 500$ repetitions.

variance with SVM-G with Weighted Cost and Grid Search than SVM-G with Weighted Cost (without Grid Search).

Next, we select only our best classifier, SVM-G with Weighted Cost and Grid Search, and compare its performance with the classifiers from benchmark study [7]. Note that in their experiments, Akbani et al also compare their method, SMOTE with Different Costs (SDC) with the regular SVM, random under-sampling (US) [38], Synthetic Minority Over-sampling Technique (SMOTE) [20], and different error costs (DEC) [61]. The results are given in Tables 5.4 and 5.5.

As pointed out in [7], the authors of DEC have not suggested any guideline for deciding the relative ratios of positive to negative cost factors. Meanwhile we adapt the setting of [7] so that the cost ratio equals the inverse of the imbalance ratio (section 5.3.2). This potential difference in cost ratio would explain how our SVM-G with Weighted Cost (see Figure 5.4 and Table 5.5) performs better than DEC, even though they are technically identical in structure. As seen in Table 5.5, our selected method outperforms the others that are

Table 5.4: The table shows the sensitivity and specificity comparison between algorithms: Support Vector Machines (SVM), Under-sampling (US), Different Error Costs (DEC), SMOTE with Different Costs (SDC).

Method	Sensitivity	Specificity
SVM	0.364	0.977
US	0.727	0.767
SMOTE	0.625	0.881
DEC	0.545	0.884
SDC	0.708	0.833
This study	**0.812**	**0.764**

Table 5.5: The table shows the G-Mean comparison between algorithms: Support Vector Machines (SVM), Under-sampling (US), Different Error Costs (DEC), SMOTE with Different Costs (SDC).

Method	G-MEAN	95% CI
SVM	0.5959695	.
US	0.7470874	.
SMOTE	0.742021	.
DEC	0.6942835	.
SDC	0.768295	.
This study	**0.784465**	**(0.784465, 0.787033)**

previously reported in [7]. Even though it is only slightly better than the SDC (1.6 % higher), it agrees with our hypothesis that employing over-sampling (SMOTE) in combining with modifying SVM cost function is unnecessary. The fact that we add Grid Search to optimize parameters C and γ does not complicate our algorithm as much as implementing over-sampling [13]. The computation time to run grid-search is fairly low since there are only two parameters to be considered. In case of larger datasets, this step can be easily parallelized (each pair (C,γ) is independent) to reduce runtime, as previously suggested in [21, 36].

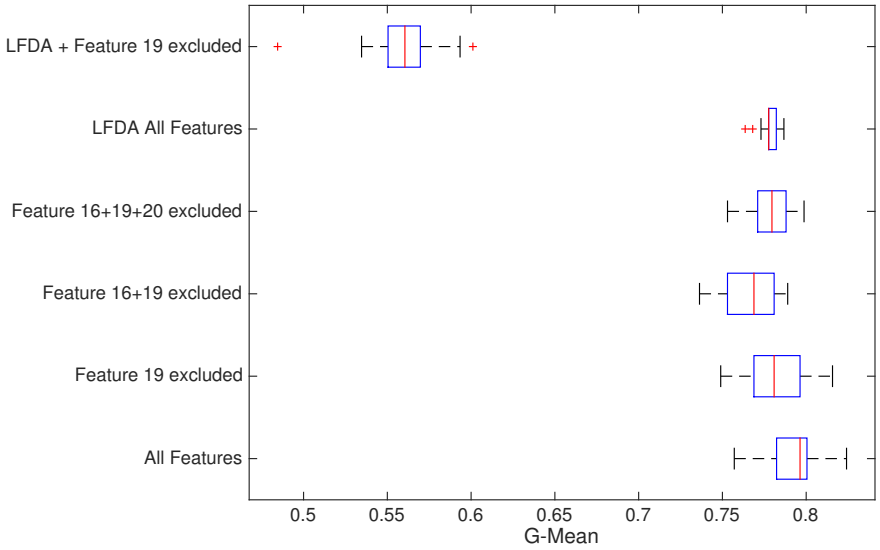

Figure 5.6: Feature Selection comparison with 10-fold CV over $N = 500$ repetitions. Number of missing values associated with features 19, 16, 20 are 67, 29, and 20 respectively (see Table 5.3).

Next, we add feature selection to our existing model. First, we remove features which contain large amount of missing values (hinting high level of noise). Then we apply the Local Fisher Discriminant Method (LFDA) similar to [21]. The results comparison of these experiments is shown in Figure 5.6. It is can be seen that as we manually remove more

[13] Over-sampling and under-sampling change the class distribution hence violate the assumptions of many Bayesian-based classifiers (section 5.2)

features, the median of G-Mean measure decreases, but the variance tends to shrink. The LFDA is then used to reduce the original 19 features to only 2 features. The variance is now at the lowest level, while G-Mean is at 77% which is only slightly less than that the original model. This is a very promising result because the ultimate goal is to reach lower out-of-sample error, and the low variance indicates that the in-sample error is a closed estimate of out-of-sample error. On the other hand, when the LFDA is applied to the dataset

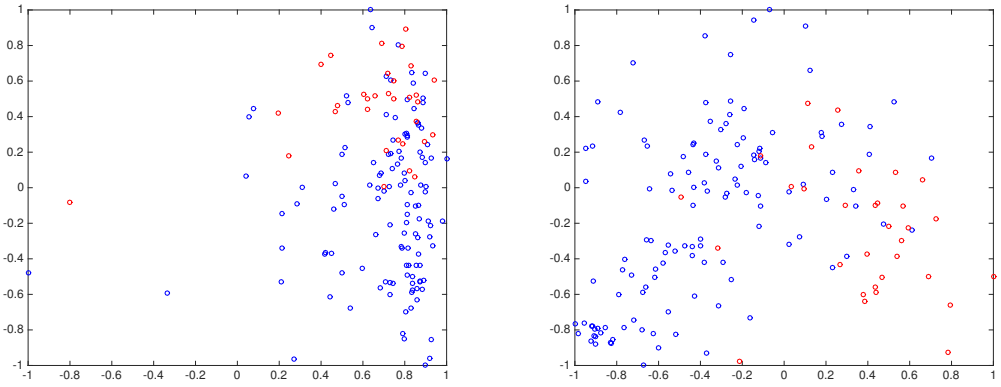

(a) Original dataset (b) Feature 19 excluded.

Figure 5.7: The scatter plots of the reduced feature subsets by LFDA.

with feature 19 excluded, the result drops considerably to about 55%. To investigate this, we plot the resulting dataset from both cases. As first, we expect the instances from the two classes are more overlapped in the second case, however it is clearly not the case, as shown in Figures 5.7a and 5.7b.

CHAPTER

6

CONCLUSION AND FUTURE WORK

6.1 Pitch Prediction

In baseball pitch prediction, strong predictive features such as speed and spin rate cannot be used. This issue forces us to find an innovative way to enhance the quality of the available feature set. Our research hence revolves around the feature selection step. We highlight some key contributions below.

- Originally, our approach developed from consideration of the factors that affect pitching decisions. For example, the pitcher/batter handedness matchup is often mentioned by sports experts as an effect [31, 35], and was originally included in our model. However, it was discovered that implementing segmentation of data based on handedness has essentially no effect on the prediction results. Thus, handedness is no longer implemented as a further splitting criterion of the model, but this component remains a considered feature. In general, unnecessary data segmentations have a

negative impact solely because they reduce the size of training and testing data for the classifiers to work with.

- The most notable is our dynamic feature selection approach which widely varies the set of features used in each pitcher-count situation. Features that yield strong prediction in some situations fail to provide any benefit in others. In fact, it is interesting to note that in the 2008 vs. 2009 prediction scheme, every feature is used in at least one situation and no feature is used in every situation. It is also interesting to note that the LDA, the most successful classification algorithm of this model is supported by our feature selection technique. In general, as a Bayesian classifier, the LDA relies on a feature independence assumption, which is realistically not satisfied. Our model survives this assumption; even though the features within each of the 6 groups are highly dependent, the final features that are chosen are highly independent.

- The model represents a significant improvement over simple guessing. It is a useful tool for batting coaches, batters, and others who wish to understand the potential pitching implications of a given game scenario. For example, batters could theoretically use this model to increase batting average, assuming that knowledge about a pitch's type makes it easier to hit. The model, for example, is especially useful in certain intense game scenarios and achieves accuracy as high as 90 percent. It is in these game environments that batters can most effectively use this model to translate knowledge into hits.

Looking forward, much can be done to improve the model.

- First, new features would be helpful. There is much game information that we did not include in our model, such as batting averages, slugging percentage per batter, stadium location, weather, and others, which could help improve the prediction accuracy of the model.

- Another potential modification is extension to multi-class classification. Currently, our model makes a binary decision and decides if the next pitch will be a fastball or not. It does not determine what kind of fastball the pitch may be. However, this task is much more difficult and would almost certainly result in a decrease in accuracy.

- Further, prediction is not limited to only the pitch type. Possible prediction objects can be pitch thrown location (specific quadrant), or pitch landing location, if for a given situation the hit occur. That information could be useful to prepare the corresponding defensive player for the impending flight of the ball.

6.2 Hepatitis Diagnosis

Our model focuses on combining three key techniques to address imbalance class: weighted cost Support Vector Machine, parameter optimization, and balance metric evaluation. These three techniques complement each other as shown in Figure 6.1. They have been shown to be efficient for providing an accurate and reliable diagnosis for Hepatitis C.

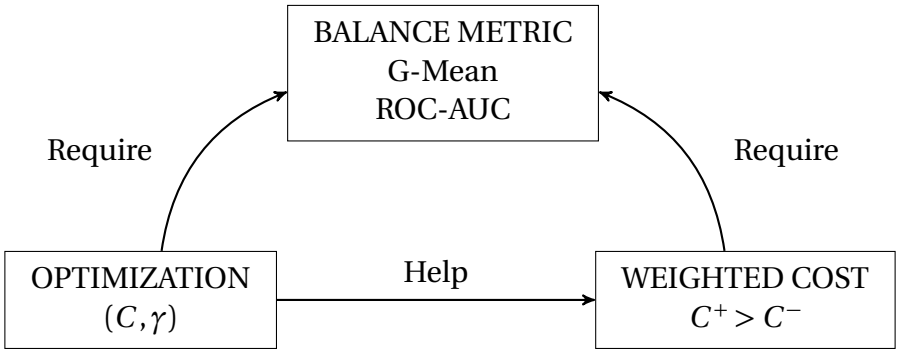

Figure 6.1: Relationship among three main components of this learning model.

We make the following specific contributions in an attempt to design and implement novel techniques to handle class imbalance:

- First, we provide empirical justification showing the existence of overfitting in previous works. For example, 15-NN is 80% accurate, but simply classifies every instances as negative. Although high accuracy can be easily attained, the poor performance in detecting positive instances remains unsolved. Such results cannot be used for disease diagnosis purpose.

- Second, we investigate methodologies that have been successfully addressed class

imbalance. We design our model by combining the weighted cost SVM with the parameters optimization via Grid Search. We also replace accuracy by other metrics such as G-Mean and ROC-AUC that are more appropriate for model evaluation of unbalanced datasets.

- Finally, learning from small datasets can yield inconsistent results even with cross validation. In response, we perform 500 simulation runs on our model and use mean value and 95% confidential interval. This is an attempt to ensure that the result comparison with the benchmark study is accurate and reliable. Our experiments show that this model can effectively use the small and unbalanced medical data to obtain trustworthy diagnosis.

Going forward, we discuss several future research directions as follows.

- Feature selection is a critical step in constructing classifier, it is in fact the center of our the contribution for the baseball pitch prediction. Our attempt of feature selection is applying LFDA to reduce the original 19 features to 2 features before feeding in the classification algorithm. While lower the classification result a little, it greatly enhances consistency with noticeable low variance. To enhance classification accuracy, one potential approach is to determine the right input-output features (currently is 19-2) for LFDA. This is however a tough task against the "Curse of Dimensionality" [1].

- There does not exist a set rule to pre-determine which kernel is best for a given dataset [1, 6]. In our experiment, we select linear kernel and Gaussian kernel because they have shown good results and run typically fast. However, authors of [23] introduce the notion of kernel alignment which indicates the degree of agreement between a kernel and a given learning task. This notion can potentially be used for kernel selection. Specifically for unbalanced datasets, the authors of [69] proposed the conformal transformation kernels. It is interesting to see whether or not this new class-boundary alignment kernel would interfere with the weighted cost SVM if they coexist in the same learning algorithm.

[1] It is common knowledge in machine learning that increasing the number of features increases the accuracy up to a certain point. Thereafter, it degrades the performance. This phenomenon is referred as the "Curse of Dimensionality"[6].

BIBLIOGRAPHY

[1] Abu-Mostafa, Y. S. et al. *Learning From Data*. AMLBook, 2012.

[2] Adeli, M. & Zarabadipour, H. "Automatic disease diagnosis systems using pattern recognition based genetic algorithm and neural networks". *Int. J. Phys. Sci. v6 i25* (2011), pp. 6076–6081.

[3] Adeli, M. et al. "New hybrid hepatitis diagnosis system based on Genetic algorithm and adaptive network fuzzy inference system". *Electrical Engineering (ICEE), 2013 21st Iranian Conference on*. IEEE. 2013, pp. 1–6.

[4] Afif, M. H. et al. "SS-SVM (3SVM): a new classification method for hepatitis disease diagnosis". *Int. J. Adv. Comput. Sci. Appl* **4** (2013).

[5] Akay, M. F. "Support vector machines combined with feature selection for breast cancer diagnosis". *Expert systems with applications* **36**.2 (2009), pp. 3240–3247.

[6] Akbani, R. *Defending against malicious nodes in closed MANETs through packet authentication and a hybrid trust management system*. The University of Texas at San Antonio, 2009.

[7] Akbani, R. et al. "Applying support vector machines to imbalanced datasets". *Machine Learning: ECML 2004*. Springer, 2004, pp. 39–50.

[8] Arlot, S. "A survey of cross-validation procedures for model selection". *Statistics Surveys* **4** (2010), pp. 40–79.

[9] Attarian, A. et al. "A Comparison of Feature Selection and Classification Algorithms in Identifying Baseball Pitches". *Int. MultiConference of Engineers and Computer Scientists 2013, Lecture Notes in Engineering and Computer Science*. Newswood Limited, 2013, pp. 263–268.

[10] Attarian, A. et al. "Baseball Pitch Classification: A Bayesian Method and Dimension Reduction Investigation". *IAENG Transactions on Engineering Sciences* (2014), pp. 392–399.

[11] Bishop, C. M. "Training with noise is equivalent to Tikhonov regularization". *Neural computation* **7**.1 (1995), pp. 108–116.

[12] Bishop, C. M. *Pattern recognition and machine learning*. Springer, 2006.

[13] Bradley, A. “The use of the area under the ROC curve in the evaluation of machine learning algorithms”. *Pattern Recogn.* **30**.7 (1997), pp. 1145–1159.

[14] Burges, C. J. “A tutorial on support vector machines for pattern recognition”. *Data mining and knowledge discovery* **2**.2 (1998), pp. 121–167.

[15] Cawley, G. C. & Talbot, N. L. “Manipulation of prior probabilities in support vector classification”. *Neural Networks, 2001. Proceedings. IJCNN'01. International Joint Conference on*. Vol. 4. IEEE. 2001, pp. 2433–2438.

[16] Central, H. *What is Ascites?* URL: `http://www.hepatitiscentral.com/hcv/whatis/ascites/`.

[17] Chabacano. *Diagram showing overfitting of a classifier*. 2008. URL: `https://commons.wikimedia.org/wiki/File:Overfitting.svg`.

[18] Chang, C.-C. & Lin, C.-J. “LIBSVM: A library for support vector machines”. *ACM Transactions on Intelligent Systems and Technology (TIST)* **2**.3 (2011), p. 27.

[19] Chang, C.-C. & Lin, C.-J. “LIBSVM: A library for support vector machines”. *ACM Transactions on Intelligent Systems and Technology* **2** (3 2011). Software available at `http://www.csie.ntu.edu.tw/~cjlin/libsvm`, 27:1–27:27.

[20] Chawla, N. V. et al. “SMOTE: synthetic minority over-sampling technique”. *Journal of artificial intelligence research* (2002), pp. 321–357.

[21] Chen, H.-L. et al. “A new hybrid method based on local fisher discriminant analysis and support vector machines for hepatitis disease diagnosis”. *Expert Systems with Applications* **38**.9 (2011), pp. 11796–11803.

[22] Courant, R. & Hilbert, D. *Methods of mathematical physics*. Vol. 1. CUP Archive, 1966.

[23] CRISTIANINI, N. “On kernel-target alignment”. *Advances in Neural Information Processing Systems* (2002).

[24] Delen, D. et al. “Predicting breast cancer survivability: a comparison of three data mining methods”. *Artificial intelligence in medicine* **34**.2 (2005), pp. 113–127.

[25] Drummond, C. & Holte, R. C. “Exploiting the cost (in) sensitivity of decision tree splitting criteria”. *ICML*. 2000, pp. 239–246.

[26] Duch, W. et al. “Minimal distance neural methods” (1998).

[27] Efron, B. “Estimating the error rate of a prediction rule: improvement on cross-validation”. *Journal of the American Statistical Association* **78**.382 (1983), pp. 316–331.

[28] Egan, J. *Signal detection theory and ROC analysis*. New York: Cognition and Perception. Academic Press, 1975.

[29] Elkan, C. “The foundations of cost-sensitive learning”. *International joint conference on artificial intelligence*. Vol. 17. 1. Citeseer. 2001, pp. 973–978.

[30] Fawcett, T. “An introduction to ROC analysis”. *Pattern recognition letters* **27**.8 (2006), pp. 861–874.

[31] Ganeshapillai, G. & Guttag, J. “Predicting the Next Pitch”. *MIT Sloan Sports Analytics Conference*. 2012.

[32] Hamilton, M. et al. “Applying Machine Learning Techniques to Baseball Pitch Prediction”. *3rd Int. Conf. on Pattern Recognition Applications and Methods*. SciTePress, 2014, pp. 520–527.

[33] Hastie, T. & Tibshirani, R. *The elements of statistical learning*. Springer, 2009.

[34] He, H., Garcia, E., et al. “Learning from imbalanced data”. *Knowledge and Data Engineering, IEEE Transactions on* **21**.9 (2009), pp. 1263–1284.

[35] Hopkins, T. & Magel, R. “Slugging Percentage in Differing Baseball Counts”. *Journal of Quantitative Analysis in Sports* **4**.2 (2008), p. 1136.

[36] Hsu, C.-W. et al. *A practical guide to support vector classification*. 2003.

[37] James, G. et al. *An introduction to statistical learning*. Springer, 2013.

[38] Japkowicz, N. “The class imbalance problem: Significance and strategies”. *Proc. of the Int. Conf. on Artificial Intelligence*. Citeseer. 2000.

[39] Jerez-Aragonés, J. M. et al. “A combined neural network and decision trees model for prognosis of breast cancer relapse”. *Artificial intelligence in medicine* **27**.1 (2003), pp. 45–63.

[40] Jilani, T. A. et al. “PCA-ANN for classification of Hepatitis-C patients”. *International Journal of Computer Applications (0975–8887)* **14**.7 (2011).

[41] Karabatak, M. & Ince, M. C. “An expert system for detection of breast cancer based on association rules and neural network”. *Expert Systems with Applications* **36**.2 (2009), pp. 3465–3469.

[42] Kubat, M., Matwin, S., et al. “Addressing the curse of imbalanced training sets: one-sided selection”. *ICML*. Vol. 97. Nashville, USA. 1997, pp. 179–186.

[43] Kubat, M. et al. “Learning when negative examples abound”. *Machine learning: ECML-97*. Springer, 1997, pp. 146–153.

[44] Lichman, M. *UCI Machine Learning Repository*. 2013.

[45] Lin, Y. et al. “Support vector machines for classification in nonstandard situations”. *Machine learning* **46**.1-3 (2002), pp. 191–202.

[46] Marckmann, G. “Recommendations for the ethical development and use of medical decision-support systems.” *MedGenMed: Medscape general medicine* **3**.3 (2001), pp. 5–5.

[47] Neshat, M. & Yaghobi, M. “Designing a fuzzy expert system of diagnosing the hepatitis B intensity rate and comparing it with adaptive neural network fuzzy system”. *Proceedings of the World Congress on Engineering and Computer Science*. Vol. 2. 2009, pp. 797–802.

[48] Ng, A. Y. “Feature selection, L 1 vs. L 2 regularization, and rotational invariance”. *Proceedings of the twenty-first international conference on Machine learning*. ACM. 2004, p. 78.

[49] Nugroho, A. S. et al. “A solution for imbalanced training sets problem by combnet-ii and its application on fog forecasting”. *IEICE TRANSACTIONS on Information and Systems* **85**.7 (2002), pp. 1165–1174.

[50] Peng, Y. *Tikz example-Kernel trick*. 2013. URL: `http://blog.pengyifan.com/tikz-example-kernel-trick/`.

[51] Peng, Y. *Tikz example-SVM trained with samples from two classes*. 2013. URL: `http://blog.pengyifan.com/tikz-example-svm-trained-with-samples-from-two-classes/`.

[52] Polat, K. & Güneş, S. “Breast cancer diagnosis using least square support vector machine”. *Digital Signal Processing* **17**.4 (2007), pp. 694–701.

[53] Provost, F. “Machine learning from imbalanced data sets 101”. *Proceedings of the AAAI 2000 workshop on imbalanced data sets*. 2000, pp. 1–3.

[54] Şahan, S. et al. “A new hybrid method based on fuzzy-artificial immune system and k-nn algorithm for breast cancer diagnosis”. *Computers in Biology and Medicine* **37**.3 (2007), pp. 415–423.

[55] Smola, A. J. et al. “The connection between regularization operators and support vector kernels”. *Neural networks* **11**.4 (1998), pp. 637–649.

[56] Swets, J. et al. “Better decisions through science”. *Scientific American* **283** (2000), pp. 82–87.

[57] Theodoridis, S. & Koutroumbas, K. *Pattern recognition*. 4th. Burlington, Mass.: Academic Press, 2009.

[58] Thoma, M. *Normal distribution for a discriminant analysis*. 2014. URL: https://commons.wikimedia.org/wiki/File:Lda-gauss-1.svg#globalusage.

[59] Vapnik, V. *The nature of statistical learning theory*. Springer Science & Business Media, 2013.

[60] Vapnik, V. N. “An overview of statistical learning theory”. *Neural Networks, IEEE Transactions on* **10**.5 (1999), pp. 988–999.

[61] Veropoulos, K. et al. “Controlling the sensitivity of support vector machines”. *Proceedings of the international joint conference on AI*. 1999, pp. 55–60.

[62] Veterans Affirs, U. D. of. *Viral Hepatitis: Commonly used terms in cirrhosis*. URL: http://www.hepatitis.va.gov/patient/complications/cirrhosis/terms.asp.

[63] Wang, B. X. & Japkowicz, N. “Boosting support vector machines for imbalanced data sets”. *Knowledge and Information Systems* **25**.1 (2010), pp. 1–20.

[64] Wang, S.-j. et al. “Empirical analysis of support vector machine ensemble classifiers”. *Expert Systems with Applications* **36**.3 (2009), pp. 6466–6476.

[65] Weinstein-Gould, J. “Keeping the Hitter Off Balance: Mixed Strategies in Baseball”. *Journal of Quantitative Analysis in Sports* **5**.2 (2009), p. 1173.

[66] West, D. & West, V. “Model selection for a medical diagnostic decision support system: a breast cancer detection case”. *Artificial Intelligence in medicine* **20**.3 (2000), pp. 183–204.

[67] West, D. et al. “Ensemble strategies for a medical diagnostic decision support system: A breast cancer diagnosis application”. *European Journal of Operational Research* **162**.2 (2005), pp. 532–551.

[68] Wikipedia. *Wikipedia Glossary of Baseball*. 2013. URL: `http://en.wikipedia.org/wiki/Glossary-of-baseball`.

[69] Wu, G. & Chang, E. Y. “Class-boundary alignment for imbalanced dataset learning”. *ICML 2003 workshop on learning from imbalanced data sets II, Washington, DC*. 2003, pp. 49–56.

[70] Xue, J.-H. & Hall, P. “Why Does Rebalancing Class-unbalanced Data Improve AUC for Linear Discriminant Analysis?” *Pattern Analysis and Machine Intelligence, IEEE Transactions on* **37**.5 (2015), pp. 1109–1112.

[71] Yasin, H. et al. “Hepatitis-C classification using data mining techniques”. *International Journal of Computer Applications* **24**.3 (2011), pp. 1–6.

[72] Zweig, M. H. & Campbell, G. “Receiver-operating characteristic ROC plots: A fundamental evaluation tool in clinical medicine”. *Clin. Chem.* **39**.4 (1993), pp. 561–577.

APPENDICES

APPENDIX

A

BASEBALL PITCH PREDICTION

A.1 Features in Groups

From the original 18 features given in Table 4.1, we generated a total of 77 features and arranged them into 6 groups as follows:

Group 1: General information of game situation

1. Inning
2. Time (day/afternoon/night)
3. Number of outs
4. Last at bat events
5. Pitcher vs. batter specific: fastball or nonfastball on previous pitch

6. Pitcher vs. batter specific: lifetime percentage of fastballs
7. Pitcher vs. batter specific: previous pitch's events
8. Numeric score of previous at bat event
9. Player on first base (true/false)
10. Player on second base (true/false)
11. Player on third base (true/false)
12. Number of base runners
13. Weighted base score

Group 2: Pitch type tendency from the past

1. Percentage of fastball thrown in previous inning
2. Percentage of fastball thrown in previous game
3. Percentage of fastballs thrown in previous at bat
4. Lifetime percentage of fastballs thrown to a specific batter over all at bats
5. Percentage of fastballs over previous 5 pitches
6. Percentage of fastballs over previous 10 pitches
7. Percentage of fastballs over previous 15 pitches
8. Percentage of fastballs over previous 20 pitches
9. Previous pitch in specific count: pitch type
10. Previous pitch in specific count: fastball or nonfastball
11. Previous 2 pitches in specific count: fastball/nonfastball combo

12. Previous 3 pitches in specific count: fastball/nonfastball combo
13. Previous pitch: pitch type
14. Previous pitch: fastball or nonfastball
15. Previous 2 pitches: fastball/nonfastball combo
16. Inning
17. Player on first base (true/false)
18. Percentage of fastballs over previous 10 pitches thrown to a specific batter
19. Percentage of fastballs over previous 15 pitches thrown to a specific batter
20. Previous 5 pitches in specific count: percentage of fastballs
21. Previous 10 pitches in specific count: percentage of fastballs
22. Previous 15 pitches in specific count: percentage of fastballs

Group 3: Pitch velocity from the past

1. Previous pitch: velocity
2. Previous 2 pitches: velocity average
3. Previous 3 pitches: velocity average
4. Previous pitch in specific count: velocity
5. Previous 2 pitches in specific count: velocity average
6. Previous 3 pitches in specific count: velocity average

Group 4: Pitch location at home plate

1. Previous pitch: horizontal position
2. Previous pitch: vertical position
3. Previous 2 pitches: horizontal position average
4. Previous 2 pitches: vertical position average
5. Previous 3 pitches: horizontal position average
6. Previous 3 pitches: vertical position average
7. Previous pitch: zone (Cartesian quadrant)
8. Previous 2 pitches: zone (Cartesian quadrant) average
9. Previous 3 pitches: zone (Cartesian quadrant) average
10. Previous pitch in specific count: horizontal position
11. Previous pitch in specific count: vertical position
12. Previous 2 pitches in specific count: horizontal position average
13. Previous 2 pitches in specific count: vertical position average
14. Previous 3 pitches in specific count: horizontal position average
15. Previous 3 pitches in specific count: vertical position average
16. Previous pitch in specific count: zone (Cartesian quadrant)
17. Previous 2 pitches in specific count: zone (Cartesian quadrant) average
18. Previous 3 pitches in specific count: zone (Cartesian quadrant) average

Group 5: Strike-result-percentage

Strike-result percentage (SRP): a metric we created that measures the percentage of strikes from all pitches in the given situation.

1. SRP of fastball thrown in the previous inning
2. SRP of fastball thrown in the previous game
3. SRP of fastball thrown in the previous 5 pitches
4. SRP of fastball thrown in the previous 10 pitches
5. SRP of fastball thrown in the previous 15 pitches
6. SRP of fastball thrown in previous 5 pitches thrown to the currently facing batter
7. SRP of nonfastball thrown in the previous inning
8. SRP of nonfastball thrown in the previous game
9. SRP of nonfastball thrown in the previous 5 pitches
10. SRP of nonfastball thrown in the previous 10 pitches
11. SRP of nonfastball thrown in the previous 15 pitches
12. SRP of nonfastball thrown in previous 5 pitches thrown to the currently facing batter

Group 6: Ball-strike combo from the similar count in the past

1. Previous pitch: ball or strike (boolean)
2. Previous 2 pitches: ball/strike combo
3. Previous 3 pitches: ball/strike combo
4. Previous pitch in specific count: ball or strike
5. Previous 2 pitches in specific count: ball/strike combo
6. Previous 3 pitches in specific count: ball/strike combo

A.2 Baseball Glossary and Info

Most of these definitions are obtained directly from [68].

1. Strike Zone: A box over the home plate which defines the boundaries through which a pitch must pass in order to count as a strike when the batter does not swing. A pitch that does not cross the plate through the strike zone is a ball.

2. Strike: When a batter swings at a pitch but fails to hit it, when a batter does not swing at a pitch that is thrown within the strike zone, when the ball is hit foul and the strike count is less than 2 (a batter cannot strike out on a foul ball, however he can fly out), when a ball is bunted foul, regardless of the strike count, when the ball touches the batter as he swings at it, when the ball touches the batter in the strike zone, or when the ball is a foul tip. Three strikes and the batter is said to have struck out.

3. Ball: When the batter does not swing at the pitch and the pitch is outside the strike zone. If the batter accrues four balls in an at bat he gets a walk, a free pass to first base.

4. Hit-By-Pitch: When the pitch hits the batters body. The batter gets a free pass to first base, similar to a walk.

5. Hit: When the batter makes contact with the pitch and successfully reaches first, second or third base. Types of hits include single (batter ends at first base), doubles (batter ends at second base), triple (batter ends at third base) and home-run.

6. Out: When a batter or base runner cannot, for whatever reason, advance to the next base. Examples include striking out (batter can not advance to first), grounding out, popping out and lining out.

7. Count: Is the number of balls and strikes during an at bat. There are 12 possible counts spanning every combination of 0-3 balls (4 balls is a walk) and 0-2 strikes (3 strikes is a strikeout).

8. Run: When a base runner crosses home plate. This is a point for that player's team. The outcome of a baseball game is determined by which team has more runs at the end of nine Innings.

9. Inning: One of nine periods of playtime in a standard game.

10. Slugging Percentage: A measure of hitter power. Defined as the average number of bases the hitter earns per at bat.

11. Batting Average: The percentage of time the batter earns a hit.

12. At Bat : A series of pitches thrown by the pitcher to one hitter resulting in a hit, a walk, or an out.

A.3 Software

All data processing and classification tasks were preformed off-line using commercial software package MATLAB (R2014a), The MathWorks Inc., Natick, MA.

1. k-NN(s, c): k-nearest-neighbors algorithm (MATLAB: *knnsearch*) with standardized Euclidean metric/Manhattan metric

2. SVM (L, G): Support Vector Machine with linear kernel and with Gaussian kernel

3. LDA: Linear discriminant analysis (MATLAB: *classify*) with linear and quadratic types.

APPENDIX

B

HEPATITIS C DIAGNOSIS

B.1 Definitions of Attributes

1. Steroid: Any group of lipids with a specific 7 carbon atom ring system [71].
2. Antiviral: It's a drug that inhibits the viral effects [71].
3. Fatigue: A state of increased discomfort and decreased efficiency due to prolonged or excessive exertion [71].
4. Malaise: Feeling of discomfort [71].
5. Anorexia: Lack or loss of appetite for foods [71].
6. Liver Big: Liver increased in size or fatty liver [71].
7. Liver Firm: Irregular hardness of liver [71].

8. Spleen Palpable: This symptom usually occur when the liver is questionably enlarged [16].

9. Spiders: Tiny veins that look like little red spiders on face, chest, and arms. They are signs of cirrhosis [62].

10. Ascites: The presence of excess fluid in the peritoneal cavity [16].

11. Bilirubin: A yellowish substance that is created by the breakdown (destruction) of hemoglobin, a major component of red blood cells [62].

12. Alk Phosphate: An enzyme exists in the blood [40].

13. Varices: Enlarged veins in the esophagus that can burst open and lead to vomiting blood or having black stool [40].

14. SGOT: Serum glutamic oxaloacetic transaminase (SGOT) is an enzyme generally exists in serum. Also, it is present in the heart [40].

15. Albumin: The chief protein of blood plasma as well as other serous solutions [40].

16. PROTIME: Prothrombin is a predecessor of thrombin which is produced in the liver [40].